

UNCLASSIFIED

AD NUMBER	
AD384237	
CLASSIFICATION CHANGES	
TO:	UNCLASSIFIED
FROM:	CONFIDENTIAL
LIMITATION CHANGES	
TO: Approved for public release; distribution is unlimited.	
FROM: Distribution authorized to U.S. Gov't. agencies and their contractors; Critical Technology; SEP 1967. Other requests shall be referred to Air Force Rocket Propulsion Lab., Research and Technology Div., Attn: RPPR-STINFO, Edwards AFB, CA 93523. This document contains export-controlled technical data.	
AUTHORITY	
AFRPL ltr dtd 18 Jan 1978 AFRPL ltr dtd 18 Jan 1978	

THIS PAGE IS UNCLASSIFIED

GENERAL DECLASSIFICATION SCHEDULE

IN ACCORDANCE WITH
DOD 5200.1-R & EXECUTIVE ORDER 11652

THIS DOCUMENT IS:

CLASSIFIED BY

DDC

Subject to General Declassification Schedule of
Executive Order 11652-Automatically Downgraded at
2 Years Intervals- DECLASSIFIED ON DECEMBER 31, 73.

BY

Defense Documentation Center
Defense Supply Agency
Cameron Station
Alexandria, Virginia 22314

THIS REPORT HAS BEEN DELIMITED
AND CLEARED FOR PUBLIC RELEASE
UNDER DOD DIRECTIVE 5200.20 AND
NO RESTRICTIONS ARE IMPOSED UPON
ITS USE AND DISCLOSURE.

DISTRIBUTION STATEMENT A

APPROVED FOR PUBLIC RELEASE;
DISTRIBUTION UNLIMITED.

SECURITY

MARKING

The classified or limited status of this report applies to each page, unless otherwise marked.

Separate page printouts MUST be marked accordingly.

THIS DOCUMENT CONTAINS INFORMATION AFFECTING THE NATIONAL DEFENSE OF THE UNITED STATES WITHIN THE MEANING OF THE ESPIONAGE LAWS, TITLE 18, U.S.C., SECTIONS 793 AND 794. THE TRANSMISSION OR THE REVELATION OF ITS CONTENTS IN ANY MANNER TO AN UNAUTHORIZED PERSON IS PROHIBITED BY LAW.

NOTICE: When government or other drawings, specifications or other data are used for any purpose other than in connection with a definitely related government procurement operation, the U. S. Government thereby incurs no responsibility, nor any obligation whatsoever; and the fact that the Government may have formulated, furnished, or in any way supplied the said drawings, specifications, or other data is not to be regarded by implication or otherwise as in any manner licensing the holder or any other person or corporation, or conveying any rights or permission to manufacture, use or sell any patented invention that may in any way be related thereto.

AD384237 19

CONFIDENTIAL

AFRPL-TR-67 -250

(UNCLASSIFIED)

**COMBUSTION MECHANISM
OF
HIGH BURNING RATE SOLID PROPELLANTS**

Contract F04611-67-C-0034

**QUARTERLY TECHNICAL REPORT AFRPL-TR-67 -250
September 1967**

**David A. Flanigan
Huntsville Division
Thiokol Chemical Corporation**

**DDC
RECEIVED
OCT 9 1967
D**

In addition to security requirements which must be met, this document is subject to special export controls and each transmittal to foreign governments or foreign nationals may be made only with prior approval of AFRPL (RPPR-STINFO), Edwards, California 93523

DOWNGRADING INFORMATION

Downgraded at 3 year intervals. Declassified after 12 years.
DOD Dir 5200.10.

DEFENSE INFORMATION

This document contains information affecting the national defense of the United States within the meaning of the Espionage Laws, Title 18 U.S.C., Sections 793 and 794. The transmission or the revelation of its contents in any manner to an unauthorized person is prohibited by law.

**Air Force Rocket Propulsion Laboratory
Research and Technical Division
Air Force Systems Command
United States Air Force
Edwards Air Force Base, California 93523**

CONFIDENTIAL

NOTICES

When U. S. Government drawings, specifications, or other data, are used for any purpose other than a definitely related Government procurement operation, the Government thereby incurs no responsibility nor any obligation whatsoever; and the fact that the Government may have formulated, furnished, or in any way supplied the said drawings, specifications, or other data, is not to be regarded by implication or otherwise, as in any manner licensing the holder or any other person or corporation, or conveying any rights or permission to manufacture, use or sell any patented invention that may be related thereto in any way.

Secrecy Order Notice, U. S. Patent Office as Modified by Permit A:
This document contains information which is subject to secrecy orders issued by the U. S. Commissioner of Patents in pursuance of Title 35, United States Code (1952), Sections 181-188.

CONFIDENTIAL

(UNCLASSIFIED)
COMBUSTION MECHANISM
OF
HIGH BURNING RATE SOLID PROPELLANTS

Contract F04611-67-C-0034

QUARTERLY TECHNICAL REPORT AFRPL-TR-67-250

David A. Flanigan

DOWNGRADING INFORMATION

Downgraded at 3 year intervals, Declassified after 12 years DOD Dir 5200.10.

DEFENSE INFORMATION

This document contains information affecting the national defense of the United States within the meaning of the Espionage Laws, Title 18 U.S.C., sections 793 and 794. The transmission or the revelation of its contents in any manner to an unauthorized person is prohibited by law.

In addition to security requirements which must be met, this document is subject to special export controls and each transmittal to foreign governments or foreign nationals may be made only with prior approval of AFRPL (RPPR-STINFO), Edwards, California 93523.

CONFIDENTIAL

CONFIDENTIAL

FOREWORD

(U) This, the third Quarterly Technical Report under Contract No. F 04611-67-C-0034, covers the work performed from 1 June through 31 August 1967. This contract with the Huntsville Division of Thiokol Chemical Corporation was initiated under Air Force Rocket Propulsion Laboratory, Research and Technology Division Project Number 3148. It is being accomplished under the technical direction of R. W. Bargmeyer, 1/Lt., USAF of the Research and Technology Division, Air Force Systems Command, United States Air Force, Edwards Air Force Base, California 93523.

(U) Dr. David A. Flanigan of Thiokol's Research and Development Department is the Principal Investigator and Mr. Carl J. Whelchel of the Project Management Directorate is Associate Program Manager for this program. Full authority for the management control of this program is the responsibility of Mr. G. F. Mangum of the Project Management Directorate. Others who cooperated in the work and in the preparation of this report are Messrs. E. C. Morganweck, C. S. Combs, C. I. Ashmore, Dr. W. D. Stephens and Mrs. E. J. Grice.

(U) This report has been assigned the Thiokol internal number 63-67(Control No. C-67-63A).

(U) This project is being accomplished as a part of the Air Force program, the overall objective of which is to tailor the burning rate of a propellant predictably and controllably to any desired level in the range from 1 to 10 inches per second. Experiments will be performed to synthesize more efficient burn rate catalysts by maximizing guideline properties determined under Contract AF04(611)-11212 toward development of an ideal catalyst. Following catalyst synthesis, each compound showing potential will be subjected to comprehensive decomposition studies and combustion mechanism evaluation with propellant ingredients.

(U) This report contains no classified information extracted from other classified documents.

STATEMENT OF APPROVAL

(U) Publication of this report does not constitute Air Force approval of the report's findings or conclusions. It is published only for the exchange and stimulation of ideas.

W. H. EBELKE, Col., USAF
Chief, Propellants Division
Air Force Rocket Propulsion Laboratory

(This page is **CONFIDENTIAL** UNCLASSIFIED)

CONFIDENTIAL

CONFIDENTIAL ABSTRACT

(C) Thiokol's program to tailor the burning rate of a propellant predictably and controllably to any desired level in the range from 1 to 10 inches per second is divided into three phases: Phase I - Synthesis of Burning Rate Catalysts, Phase II - Decomposition Studies and Evaluation of Catalysts and Phase III - Decomposition of Advanced Oxidizers, Fuels, and Binders. Experiments will be performed to synthesize more efficient burn rate catalysts by maximizing already determined guideline properties toward development of an ideal catalyst under Phases I and II. Following catalyst synthesis, each compound showing potential will be subjected to comprehensive decomposition studies and combustion mechanism evaluation with propellant ingredients. Thermogravimetric analyses of catalysts mixed with HC polymer show that none of the catalysts tested appear to catalyze the decomposition of HC polymer. Propellants formulated with the copper (I) complex, the copper (II) complex and the cobalt (II) complex of β -ferrocenyl- β -oxo-propionaldehyde demonstrated burning rates higher than that of similar propellant containing n-butyl ferrocene [PLASTISCAT-IV(R)] at the 2 percent level. An analysis to relate subsurface heating to changes in ammonium perchlorate crystal structure was conducted. It was shown that if the concept of a constant surface temperature is valid and if the extrapolated value of thermal diffusivity is accurate to within 10 percent, the surface temperature of burning ammonium perchlorate is $440 \pm 30^\circ\text{C}$.

CONFIDENTIAL

CONFIDENTIAL

TABLE OF CONTENTS

	<u>Page</u>
SECTION I	
INTRODUCTION	1
SECTION II	
EXPERIMENTAL ACCOMPLISHMENTS	3
1. Phase I - Synthesis of Burning Rate Catalysts	3
2. Phase II - Decomposition Studies and Catalyst Evaluation	9
a. Catalyst Compatibility Studies	9
b. Burning Rate Studies	20
SECTION III	
CONCLUSIONS	27
APPENDIX A	
Analysis to Relate Subsurface Heating to Changes in Ammonium Perchlorate Crystal Structure	29

LIST OF TABLES

<u>Number</u>	
I.	Thermogravimetric Analysis of Catalysts Mixed with HC Polymer
	11
II.	Catalyst Compatibility
	13

CONFIDENTIAL

(This page is UNCLASSIFIED)

CONFIDENTIAL

LIST OF FIGURES

<u>Number</u>		<u>Page</u>
1.	(C) Differential Thermal Analyses of 2-methoxyethyl ferrocenyl ether, hydroxymethyl ferrocene, 2-methylthioethyl ferrocenylmethyl ether and AFB 1-Poly.	14
2.	(C) Differential Thermal Analyses of dimethyl ferrocenylmethyl ammonium nitrate, 2,2' bis(dimethylaminomethyl) ferrocene dipicrate, and dimethylaminomethyl ferrocene picrate.	15
3.	(C) Differential Thermal Analyses of methyl-4-oxo-4-ferrocenylbutyrate, acetylferrocene ethylthioketal, and cobalt (II) complex of β -ferrocenyl- β -oxo-propionaldehyde.	16
4.	(C) Differential Thermal Analyses of ethylthiomethyl ferrocene, dimethyl ferrocenylmethyl ammonium fluoride, and 1-ferrocenylmethoxy-3-butanone	17
5.	(C) Differential Thermal Analyses of Manganese (II) complex of β -ferrocenyl-oxo-propionaldehyde, acetonylthiomethyl ferrocene, and isopropyl ferrocenylmethyl ether.	18
6.	(C) Differential Thermal Analyses of 2,2-bis(acetyl) ethyl ferrocene, 2-methoxyethyl β -ferrocenoyl-propionate, and 2-chloroethyl ferrocenylmethyl ether	19
7.	(C) Comparison of the Burning Rate of Propellant Catalyzed with PLASTISCAT-IV(R) and Copper (II) Complex of β -ferrocenyl- β -oxo-propionaldehyde.	22
8.	(C) Comparison of the Burning Rate Characteristics of Propellant Catalyzed with n-butyl ferrocene [PLASTISCAT-IV(R)] and a Mixture of 1,1'-di(methoxymethyl)ferrocene and 1-hydroxymethyl-1'-methoxymethyl ferrocene	23
9.	(C) Comparison of the Burning Rate of Propellant Catalyzed with PLASTISCAT-IV(R), Copper (I) complex of β -ferrocenyl- β -oxo-propionaldehyde, and Dimethylaminomethyl ferrocenium Picrate.	24

CONFIDENTIAL

List of Figures (Continued)

<u>Number</u>		<u>Page</u>
10. (C)	Comparison of the Burning rate of Propellant Catalyzed with n-butyl ferrocene [PLASTISCAT-IV(R)] and n-butylthiomethyl ferrocene	25
11. (C)	Comparison of the Burning Rate of Propellant Catalyzed with PLASTISCAT-IV(R), Cobalt (III) complex of β -ferrocenyl- β -oxo-propionaldehyde, and Manganese (II) complex of β -ferrocenyl- β - oxo-propionaldehyde.	26

CONFIDENTIAL

CONFIDENTIAL

SECTION 1

INTRODUCTION

(U) The objective of this program is to tailor the burning rate of a propellant predictably and controllably, to any desired level in the range from 1 to 10 inches per second. Ballistic and mechanical properties of propellants studied will be maintained at the state-of-the-art standards of current Minuteman propellant.

(C) Thiokol's approach to obtain the program objective will be through the continued investigation of iron compound effects on the aluminum-ammonium perchlorate-polybutadiene binder system. It is also designed to systematically evaluate new propellant ingredients as to their effect on burning rate and the related effect on combustion mechanism. New materials which will be evaluated are hydroxyl-ammonium perchlorate, hydrazine dperchlorate and nitronium perchlorate oxidizers; aluminum hydride, beryllium, beryllium hydride fuels; P-BEP, NFPA polymers, and TVOPA plasticizer. The data and conclusions reached under Contract AF04(611)-11212 will be used as a base line guide for the work to be accomplished under this program.

(U) The planned program consists of three major areas: synthesis, evaluation, and advanced ingredient studies. It is designed to progress in a logical manner so that the most promising materials receive the more extensive evaluation and the less desirable materials are discarded at an early date. The three phases of the program are:

(U) Phase I - Synthesis of Burning Rate Catalysts

(U) Burning rate catalysts will be synthesized for use in the AP/Al/PB propellant system. Prior knowledge as a propulsion contractor and the data obtained from Contract AF04(611)-11212 will serve as base line guides. As a new material is synthesized, it will be evaluated in Phase II.

(U) Phase II - Decomposition Studies and Evaluation of Catalysts

(U) An evaluation of the compatibility of the candidate catalysts with other propellant ingredients will be accomplished upon completion of synthesis, elemental characterization, and physical property determination of each candidate material. Data obtained in this phase will allow recommendations to be made relative to the development of new burning rate catalysts and the development of high burning rate propellants utilizing the improved catalyst.

CONFIDENTIAL

CONFIDENTIAL

(U) Phase III - Decomposition of Advanced Oxidizers, Fuels, and Binders

(U) Phase III effort will be directed toward obtaining a basic fundamental knowledge of the decomposition of advanced fuels, oxidizers, and binders. Laboratory test data will be utilized to postulate a burning mechanism of the advanced ingredient and a comparison made with that of conventional propellant ingredients.

(U) This report covers work performed for the period 1 June through 31 August 1967 under Contract F 04611-67-C-0034. Effort to date has been concerned solely with Phases I and II, which are being conducted concurrently. Phase III will be initiated after the completion of Phases I and II.

CONFIDENTIAL

SECTION II

EXPERIMENTAL ACCOMPLISHMENTS

(U) Based on the results of effort expended under Contract AF04(611)-11212, the experiments under this program will be directed toward the synthesis and characterization of more efficient burn rate catalysts.

(U) 1. Phase I - Synthesis of Burning Rate Catalysts

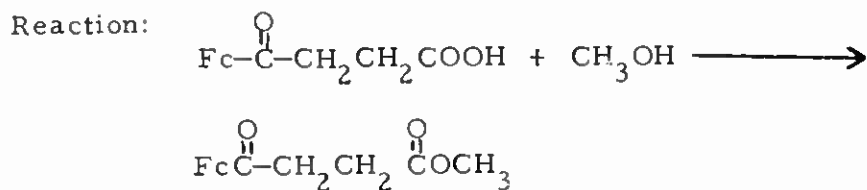
(U) The guidelines for synthesis of more efficient burn rate catalysts have been derived from effort conducted under the above contract and are listed below:

High iron content
Wide liquid range
Readily oxidizable
Compatible with other propellant ingredients
Maximum fuel content (heat release on oxidation)

(U) The synthesis of newer burn rate catalysts will be directed toward maximizing the aforementioned properties into the ideal catalyst.

(U) Effort performed in this area of research during this reporting period is presented in subsequent paragraphs.

(C) Esterification of β -ferrocenoylpropionic acid with methanol gave methyl β -ferrocenoyl propionate in 80 percent yield.

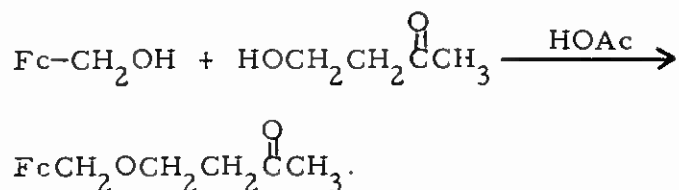


(C) Reaction of hydroxymethyl ferrocene with 4-hydroxy-2-butanone using acetic acid catalyst gave 4-ferrocenylmethoxy-2-butanone in 77 percent yield.

CONFIDENTIAL

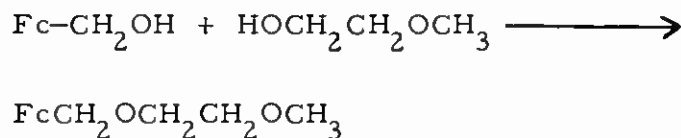
CONFIDENTIAL

Reaction:



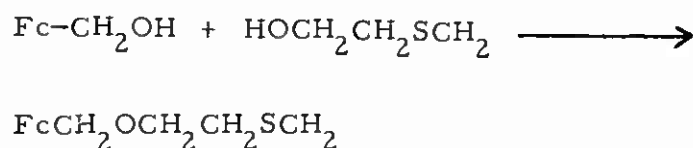
(C) Substitution of 2-methoxyethanol for 4-hydroxy-2-butanone gave 1-methoxy-2-(ferrocenylmethoxy)-ethane in 70 percent yield.

Reaction:



(C) Use of methylthioethanol gave 1-methylthio-2-ferrocenylmethoxyethane, in 50 percent yield.

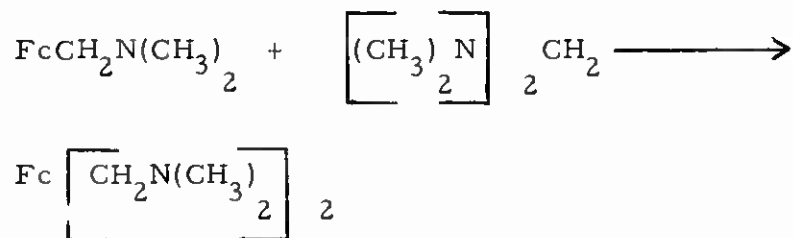
Reaction:



(U) Several solid derivatives of dimethylaminomethyl ferrocene have been synthesized. The perchlorate, nitrate, picrate, iodide, bromide and fluoride salts have been prepared either through neutralization or metathesis reactions.

(C) Treatment of N, N-dimethylaminomethyl ferrocene with bis-dimethylaminomethane gave 1, 1'-bis (dimethylaminomethyl) ferrocene in 28 percent yield.

Reaction:



(U) The structural assignments of the above catalyst were confirmed by infrared analysis.

CONFIDENTIAL

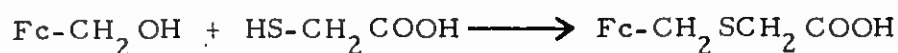
(C) The reaction between hydroxymethyl ferrocene and mercaptoacetic acid gave α -(ferrocenylmethylthio)-acetic acid in 75 percent yield.

Elemental analysis:

	Carbon (%)	Hydrogen (%)
Calculated	53.81	4.86
Found	53.91	5.27

Melting point: 124 - 125°C

Reaction:



(C) Esterification of α -(Ferrocenylmethylthio)-acetic acid with methanol gave methyl -(Ferrocenylmethylthio)acetate, according to the following:

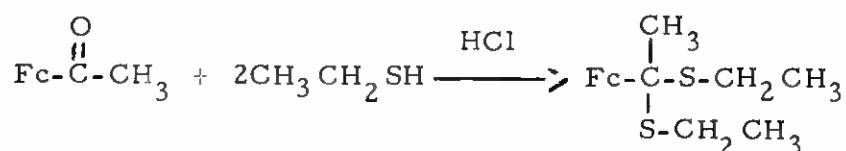
Reaction:



(C) The reaction of acetyl ferrocene with ethyl mercaptan gave acetyl ferrocene ethylthioketal in 51 percent yield.

Melting point: 40 - 41°C

Reaction:



(C) An unsuccessful attempt was made to prepare a keto-ester-sulfide ferrocene compound by reacting α -(ferrocenylmethylthio)-propionic acid with 4-hydroxy-2-butanone.

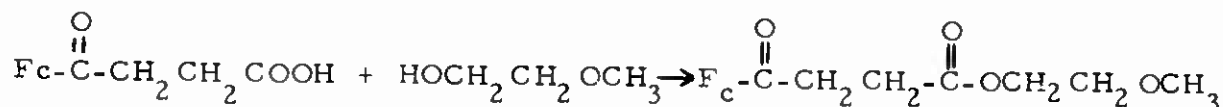
CONFIDENTIAL

CONFIDENTIAL

(C) A ferrocene compound containing keto-ester and ether groups was successfully prepared in 30 percent yield by reacting β -ferrocenylpropionic acid with 2-methoxyethanol, which gave 2-methoxyethyl - β -ferrocenoyl propionate.

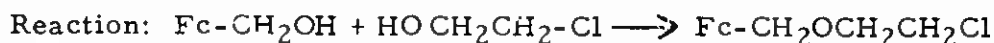
Melting point: 47 - 49°C

Reaction:



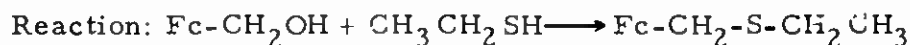
(C) The reaction of hydroxymethyl ferrocene with 2-chloroethanol gave 2-chloroethoxymethyl ferrocene in 50 percent yield.

Elemental Analysis:	<u>Carbon</u> (%)	<u>Hydrogen</u> (%)
Calculated -	56.1	5.4
Found -	57.9	5.42



(C) The reaction of hydroxymethyl ferrocene with ethyl mercaptan gave ethylthiomethyl ferrocene in 40 percent yield.

Elemental Analysis:	<u>Carbon</u> (%)	<u>Hydrogen</u> (%)
Calculated -	60.0	6.16
Found -	60.22	6.33

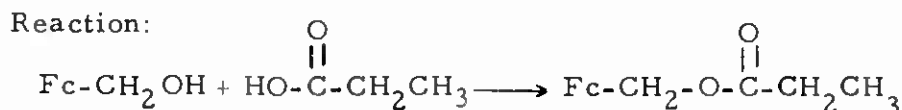


(C) The reaction of hydroxymethyl ferrocene with propionic acid gave ferrocenylmethylpropionate in 35 percent yield.

CONFIDENTIAL

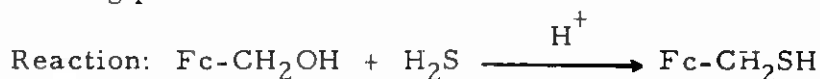
Elemental Analysis:	Carbon (%)	Hydrogen (%)
Calculated	- 61.8	5.88
Found	- 62.2	5.63

Melting point: 55 - 57°C

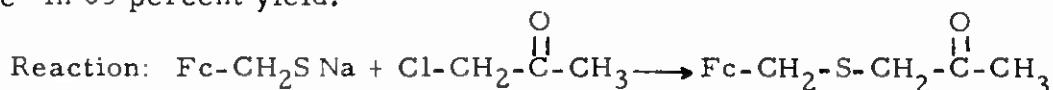


(C) The reaction of hydroxymethyl ferrocene with hydrogen sulfide gave ferrocenylmethyl mercaptan in 90 percent yield.

Melting point: 53 - 55°C



(C) The reaction of ferrocenylmethylmercaptan with chloro-2-propanone in sodium hydroxide solution gave 1-(ferrocenylmethylthio)-2-propanone in 65 percent yield.



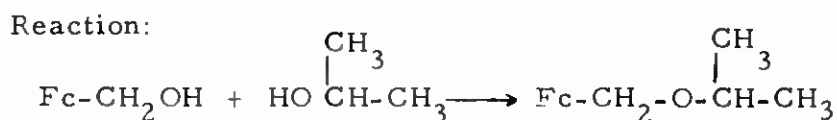
(C) The reaction of ferrocenylmethylmercaptan with allyl bromide in sodium hydroxide solution gave allylthiomethyl ferrocene in 80 percent yield.

Reaction:



(C) The reaction of hydroxymethyl ferrocene with isopropyl alcohol gave isopropoxymethyl ferrocene in 70 percent yield.

Melting point: 33 - 34°C

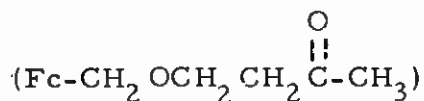


(C) An unsuccessful attempt was made to prepare a keto-ester-sulfide ferrocene compound by reacting β -ferrocenoylpropionic acid with 2-methylthioethanol. The previously attempted esterification of α -(ferrocenylmethylthio)-acetic acid with 4-hydroxy-2-butanone was also unsuccessful.

CONFIDENTIAL

(U) Physical constants and elemental analysis for previously reported catalysts were determined during this report period and are shown below.

(C) 4-Ferrocenylmethoxy-2-butanone

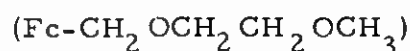


Elemental analysis:

	<u>Carbon</u> (%)	<u>Hydrogen</u> (%)
Calculated	63.0	6.4
Found	63.03	6.42

Melting point: 15 - 17°C

(C) 1-methoxy-2-ferrocenylmethoxyethane



Elemental analysis:

	<u>Carbon</u> (%)	<u>Hydrogen</u> (%)
Calculated	61.4	6.57
Found	61.59	6.71

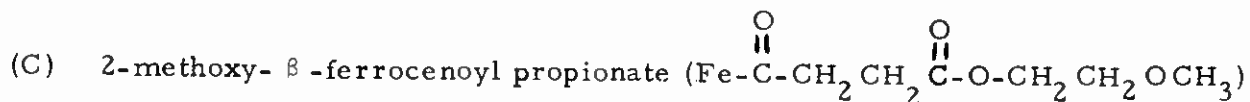
Melting point: 20 - 22°C

(C) The melting point of methoxymethyl ferrocene ($\text{Fc}-\text{CH}_2\text{OCH}_3$) was determined to be: 6 - 8°C.

(C) Acetyl ferrocene ethylthioketal $[\text{Fc}-\overset{\text{CH}_3}{\underset{|}{\text{C}}}(-\text{S}-\text{CH}_2-\text{CH}_3)_2]$

Elemental analysis:

	<u>Carbon</u> (%)	<u>Hydrogen</u> (%)
Calculated	57.5	6.6
Found	57.77	6.77



Elemental analysis:

	<u>Carbon</u> (%)	<u>Hydrogen</u> (%)
Calculated	59.4	5.82
Found	59.5	5.84

The melting point of allyloxy methyl ferrocene ($\text{Fe}-\text{CH}_2\text{OCH}_2\text{CH}=\text{CH}_2$) was determined to be -11 to -10°C .

(U) 2. Phase II - Decomposition Studies and Catalyst Evaluation

(U) An evaluation of the compatibility of the candidate catalysts with other propellant ingredients will be accomplished upon completion of synthesis, elemental characterization and physical property determination of each candidate catalyst. Following the compatibility studies, the actual effectiveness of the candidate catalysts will be measured by determining the propellant processing characteristics as well as the burning rate.

(U) a. Catalyst Compatibility Studies

(C) Nineteen newly synthesized catalysts were evaluated by differential thermal analysis (DTA) during this report period. These catalysts were:

2-methoxyethyl ferrocenyl ether
 hydroxymethyl ferrocene
 2-methylthioethyl ferrocenylmethyl ether
 A ferrocene polymer of undetermined structure (AFB 1-Poly)
 dimethyl ferrocenylmethyl ammonium nitrate
 2, 2' bis(dimethylaminomethyl) ferrocene dipicrate
 dimethylaminomethyl ferrocene picrate
 methyl-4-oxo-4-ferrocenylbutyrate
 acetyl ferrocene ethylthioketal
 cobalt (II) complex of β -ferrocenyl- β -oxo-propionaldehyde
 ethylthiomethyl ferrocene
 dimethyl ferrocenylmethyl ammonium fluoride
 1-ferrocenylmethoxy-3-butanone

CONFIDENTIAL

manganese (II) complex of β -ferrocenyl- β -oxo-propionaldehyde
acetonylthiomethyl ferrocene
isopropyl ferrocenylmethyl ether
2, 2-bis (acetyl) ethyl ferrocene
2-methoxyethyl- β -ferrocenoylpropionate
2-chloroethyl ferrocenylmethyl ether

These data, which are presented on Figures 1 through 6, show that 2-methylthioethyl ferrocenylmethyl ether, dimethyl ferrocenylmethyl ammonium nitrate, the cobalt (II) complex of β -ferrocenyl- β -oxo-propionaldehyde, and the manganese (II) complex of β -ferrocenyl- β -oxo-propionaldehyde appear to affect significantly the thermal decomposition of ammonium perchlorate.

(C) Several previously synthesized catalysts were mixed with HC polymer and subjected to thermal gravimetric analysis (TGA). About 0.01 gram of each catalyst was mixed with 0.19 gram HC polymer, producing a five percent (weight) catalyst mixture. HC polymer without any added catalyst was also subjected to TGA. Temperatures at the start and at the end of weight loss are given in Tables I and II. The lower temperatures at start of weight loss for the catalyst/HC polymer mixtures are attributed to volatilization of the catalysts. The catalyst/HC polymer mixtures indicated by (a) in the tables apparently cured to a rubber during the pyrolysis. The first sample of bis(α -ferrocenylethyl) ether/HC polymer was examined microscopically after being thrown from the sample tube. It was a hard rubber containing numerous bubbles of gas. The audible "pop" accompanied by a sudden weight loss, noted for this and some of the other samples, is therefore attributed to sudden release of decomposition gases by the cured HC polymer. Apparently catalysts containing an ether linkage and some other structures react to cure the HC polymer at temperatures around 360°C. None of the compounds tested appeared to catalyze the decomposition of HC polymer. This is evidenced by the fact that the temperature at end of weight loss was nearly the same in all of the catalyst/HC polymer mixtures.

(C) Recently synthesized catalysts have been tested for compatibility with HC polymer and MAPO. Small scale mixes were prepared and examined under the microscope at ambient temperature and resulting discoloration, dissolving of the catalyst, evolution of gas or heat, etc., was noted. These samples were then placed in a 160 \pm 1°F oven for 24 hours, after which they were re-examined microscopically. Control tests of HC polymer and MAPO containing no catalysts were also run. Results are given in Table III. All of the catalysts tested appear to be compatible with HC polymer and MAPO at ambient temperature. However, under the 160°F conditions only 2-methylthioethyl ferrocenylmethyl ether, 2-methoxyethyl ferrocenylmethyl ether, and dimethyl ferrocenylmethyl ammonium nitrate were compatible with both HC polymer and MAPO.

TABLE I

THERMOGRAVIMETRIC ANALYSIS OF CATALYSTS MIXED WITH HC POLYMER (U)

Catalyst	Temperature at Start Of Weight Loss		Temperature at End Of Weight Loss	
	(°C)		(°C)	
None	330		565	
Copper (I) complex of β -ferrocenyl- β -oxo-propionaldehyde	270		580	
Bis (α -ferrocenylethyl) ether	300 ^(a)		---	^(b)
(Rep at of above)	265 ^(a)		550	
Dimethylaminomethyl ferrocene	250		570	
Ethoxymethyl ferrocene	235 ^(a)		575	
Allyl ferrocenoate	240		570	
Methoxymethyl ferrocene	250 ^(a)		570	
Allyloxymethyl ferrocene	235 ^(a)		565	
1,3-diferrocenyl-1 oxo-2-propene	270		600	
1,3-diferrocenyl-1,3-propanedione	270		590	
Methyl β -(ferrocenylmethylthio) propionate	320		605	
Mixture (60:40) of 1,1'-di(methoxymethyl) ferrocene and 1-hydroxymethyl-1'-methoxymethyl ferrocene	255		625	
2-methoxyethyl ferrocenoate	300		565	

TABLE I (Continued)

Catalyst	Temperature at Start		Temperature at End	
	of Weight Loss		Of Weight Loss	
	(°C)		(°C)	
None				565
Bis-ferrocenylmethyl ether	330	(a)		555
Ferrocenylmethyl ferrocenoate	325			570
Hydroxymethyl ferrocene	280	(a)		525
n-butylthiomethyl ferrocene	270			575
poly-[bis (methylthiomethyl) ferrocene]	295			590
1, 1'-di (methoxymethyl) ferrocene	340	(a)		565
Dimethylaminomethyl ferrocene picrate	280			590
2-methoxyethyl ferrocenylmethyl ether	245			580
Methyl ferrocenylacetate	270			595
n-propyl ferrocenoate	290			590
Dimethylaminomethyl ferrocene	320	(a)		605
Cobalt (II) complex of β -ferrocenyl- β -oxo-propionaldehyde	320			625
2-methylthioethyl ferrocenylmethyl ether	295			600
Trimethoxy iron	180			590
Propargyl ferrocenoate	280			585
Dimethyl ferrocenylmethyl ammonium nitrate	205	(a)		570

a. These samples exhibited sudden weight losses accompanied by an audible "pop".

b. Sample thrown from tube at 360°C.

CONFIDENTIAL

TABLE II
CATALYST COMPATIBILITY (U)

Catalyst	HC Polymer		MAPO	
	Ambient	160°F(a)	Ambient	160°F(a)
Dimethylaminomethyl ferrocene picrate	insoluble	no change	soluble	cured
2-methylthioethyl ferrocenylmethyl ether	insoluble	no change	insoluble	no change
2-methoxyethyl ferrocenylmethyl ether	miscible	no change	miscible	no change
Hydroxymethyl ferrocene	insoluble	soluble	soluble	cured
2, 2' bis (dimethylaminomethyl) ferrocene dipicrate	insoluble	no change	partially soluble	cured
Cobalt (II) complex of β -ferrocenyl- β -oxo-propionaldehyde	insoluble	cured	insoluble	no change
Dimethyl ferrocenylmethyl ammonium nitrate	insoluble	no change	insoluble	no change

a. Samples placed in 160°F oven for 24 hours.

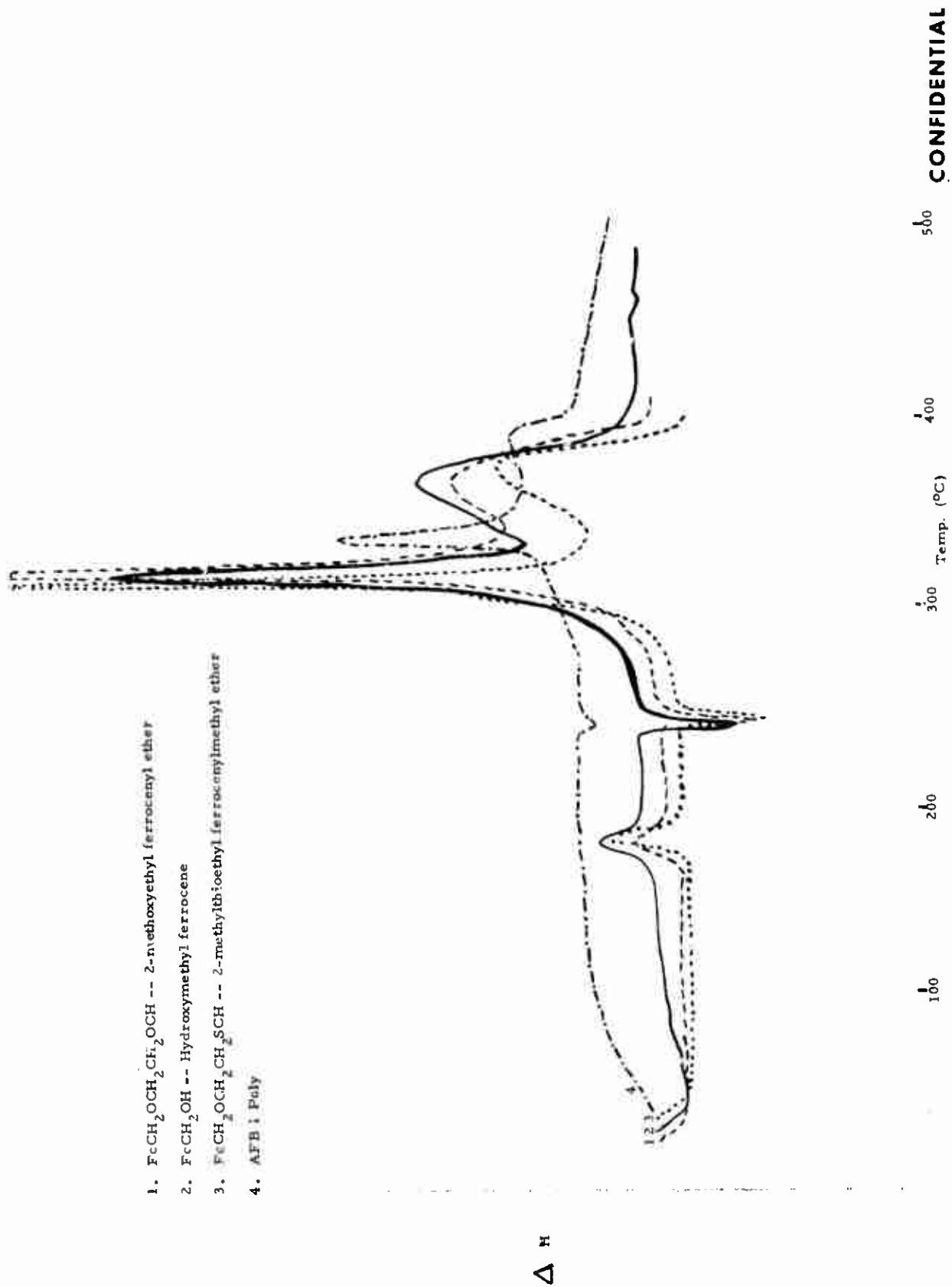


Figure 1. (C) Differential Thermal Analyses of 2-methoxyethyl ferrocenyl ether, hydroxymethyl ferrocene, 2-methylthioethyl ferrocenylmethyl ether and AFB 1-Poly.

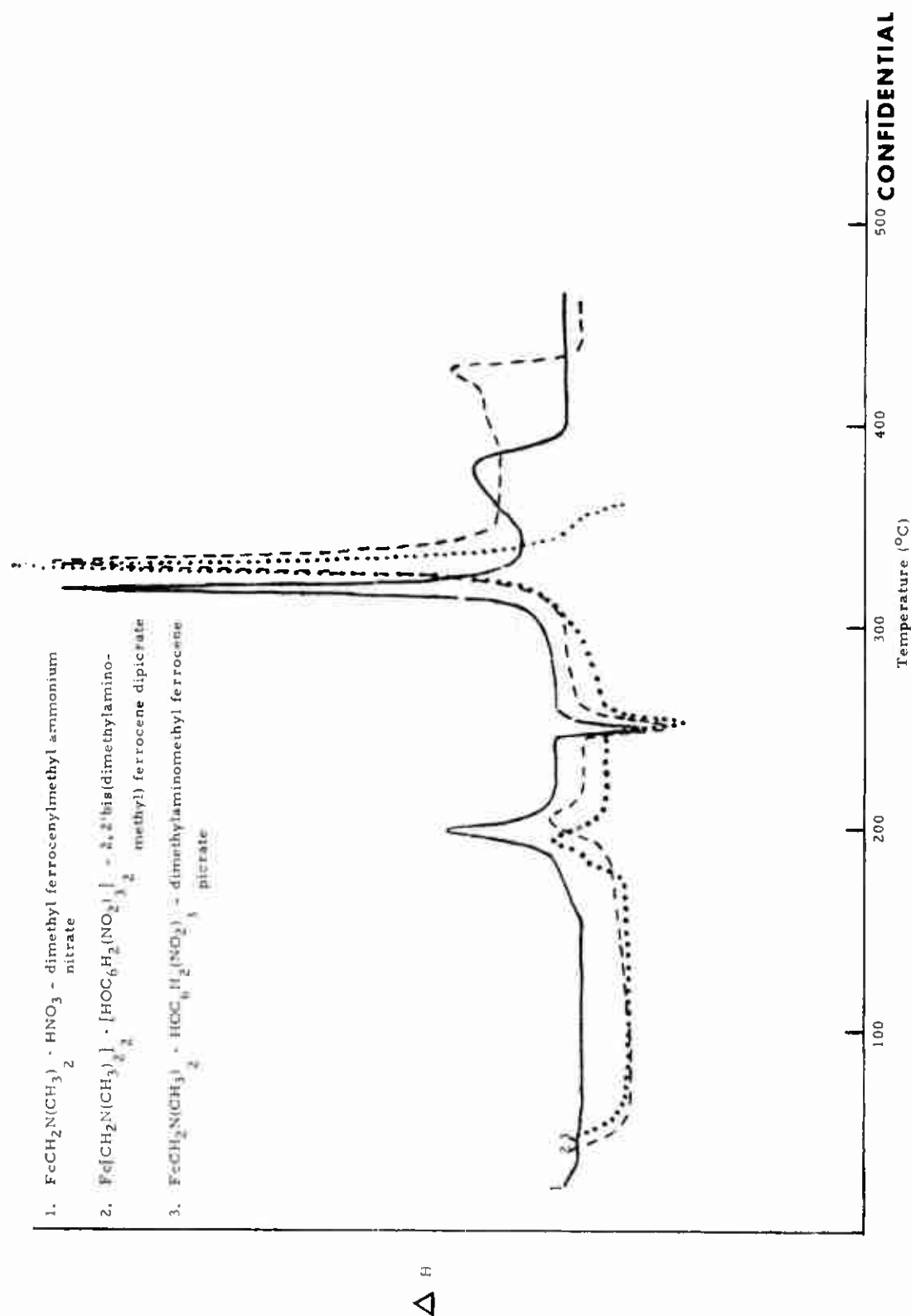


Figure 2. (C) Differential Thermal Analyses of dimethyl ferrocenylmethyl ammonium nitrate, 2,2'-bis(dimethylaminomethyl) ferrocene dipicrate, and dimethylaminomethyl ferrocene picrate.

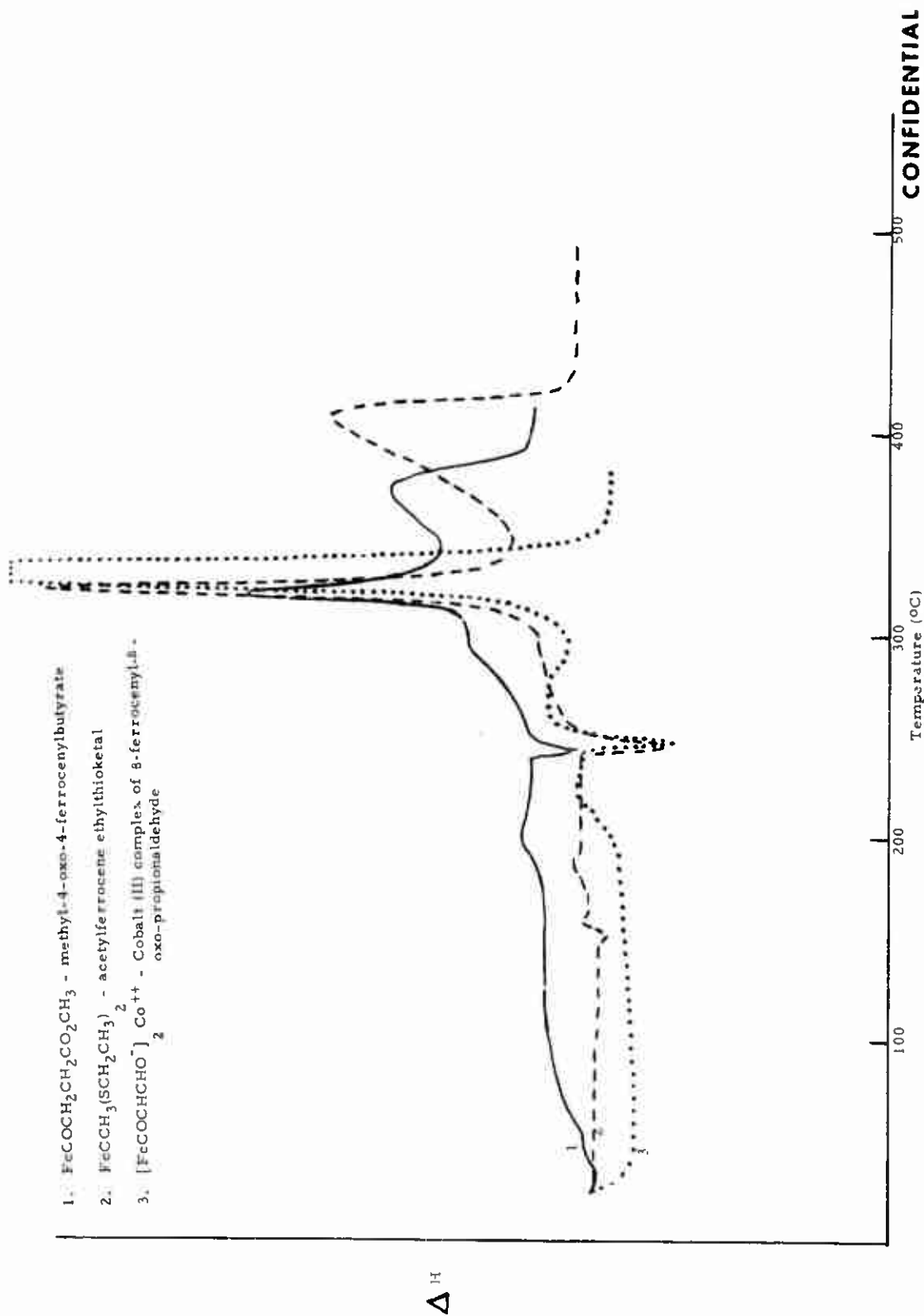


Figure 3 (C) Differential Thermal Analyses of methyl-4-oxo-4-ferrocenylbutyrate, acetylferrocene ethylthioether, and cobalt (II) complex of 8-ferrocenyl-8-oxo-propionaldehyde.

CONFIDENTIAL

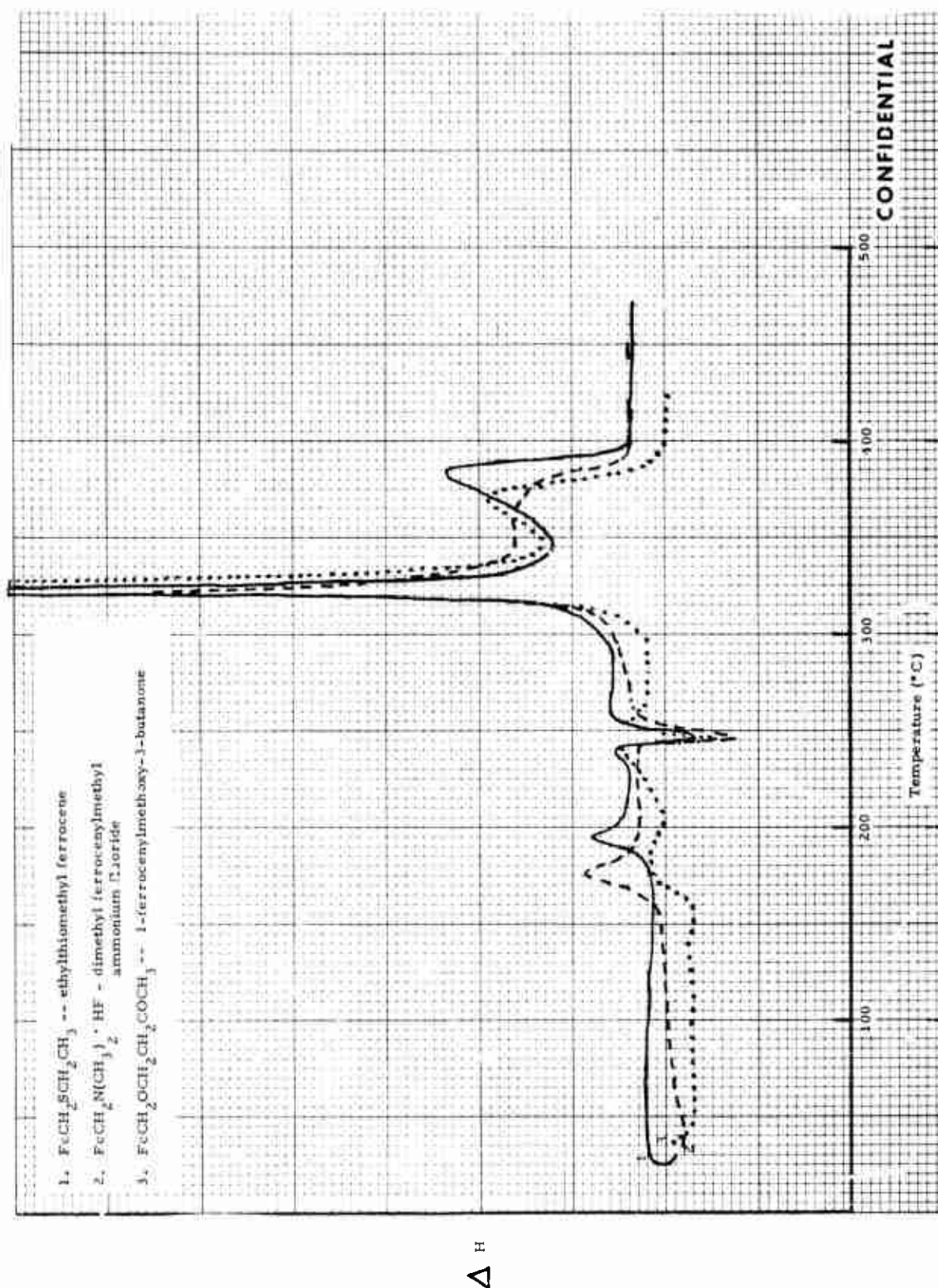


Figure 4. (C) Differential Thermal Analyses of ethylthiomethyl ferrocene, dimethyl ferrocenylmethyl ammonium fluoride, and 1-ferrocenylmethoxy-3-butanone.

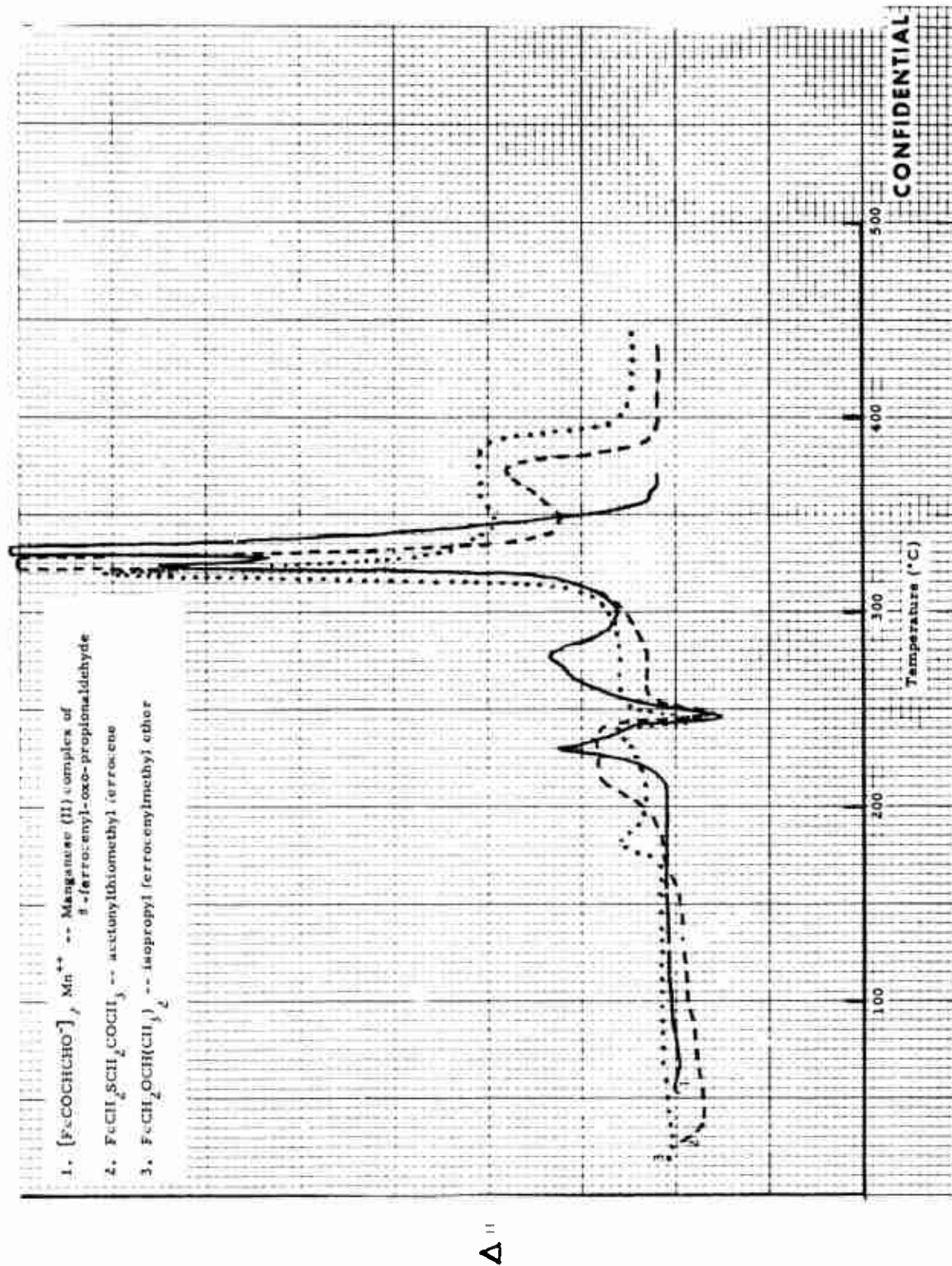


Figure 5. (C) Differential Thermal Analyses of Manganese (II) complex of β -ferrocenyl-oxo-propionaldehyde, acetonylthiomethyl ferrocene, and isopropyl ferrocenylmethyl ether.

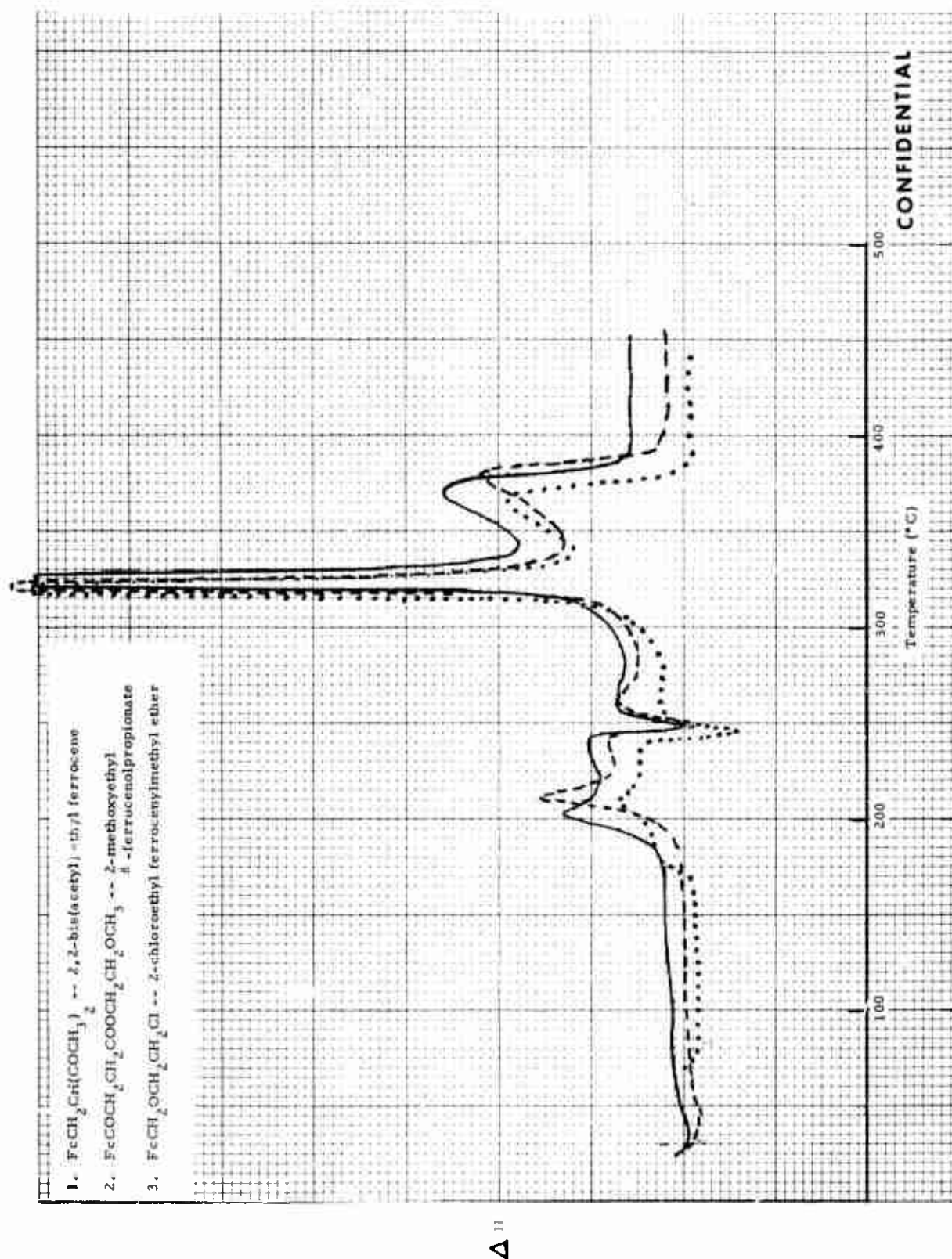


Figure 6. (C) Differential Thermal Analyses of 2,2-bis(acetyl)ethyl ferrocene, 2-methoxyethyl 8-ferrocenylpropionate, and 2-chloroethyl ferrocenylmethyl ether.

CONFIDENTIAL

(U) b. Burning Rate Studies

(C) A 1,000 gram batch of HC propellant without burning rate catalyst or curing agent was prepared, and 100 gram batches of propellant containing burn rate catalyst and curing agent were prepared from the master batch. Strands were cut from the cured propellant and burning rates were determined. Catalysts evaluated were:

copper (II) complex of β -ferrocenyl- β -oxo-propionaldehyde
60:40 mixture of 1, 1-di(methoxymethyl) ferrocene and
1-hydroxymethyl-1'-methoxymethyl ferrocene
copper (I) complex of β -ferrocenyl- β -oxo-propionaldehyde
dimethylaminomethyl ferrocene picrate
n-butylthiomethyl ferrocene
cobalt (II) complex of β -ferrocenyl- β -oxo-propionaldehyde
manganese (II) complex of β -ferrocenyl- β -oxo-propionaldehyde

(C) Addition of copper (II) complex followed by MAPO addition and 15 minutes of vacuum mixing resulted in a viscosity of 60 to 65 kilopoise at 145°F. The addition of the above ether mixture gave a viscosity reduction to 20 kilopoise. No viscosity reduction was experienced with addition of either the copper (I) complex, dimethylaminomethyl ferrocene picrate, the cobalt (II) complex or the manganese (II) complex. Addition of n-butylthiomethyl ferrocene to the propellant mix effected a viscosity reduction to the 20 to 25 kilopoise range.

(C) Propellant made with the copper (II) complex gave a very soft cure after approximately one month. A good cure was exhibited by the propellant made with the ether mixture after four-and-one-half-days. Propellant made with the copper (I) complex gave a soft cure after approximately one month. The degree of cure exhibited was similar to that for the copper (II) complex of the same compound. Dimethylaminomethyl ferrocene picrate gave propellant that was hard and crumbly. A good propellant cure was produced by n-butylthiomethyl ferrocene. Propellant made with the cobalt (II) complex cured in about three days and was hard and crumbly. It is probable that the incompatibility of the cobalt (II) complex with HC polymer at elevated temperatures was the cause of this "hard" cure. Propellant made with the manganese (II) complex gave a good propellant cure.

CONFIDENTIAL

(C) A comparison of the burning rate of propellant formulated with these complexes and with n-butyl ferrocene [PLASTISCAT-IV^(R)] (Figures 7 through 11) show the following:

Copper (II) complex	Higher over entire pressure range
60:40 ether mixture	Slightly higher over entire pressure range
Copper (I) complex	Considerably higher throughout pressure range of 400 to 1200 psig
Dimethylaminomethyl ferrocene picrate	Considerably below
n-butylthiomethyl ferrocene	Considerably below
Cobalt (II) complex	Somewhat higher throughout pressure range of 400 to 1200 psig
Manganese (II) complex	Somewhat lower throughout pressure range of 400 to 1200 psig

These data also show that burning rates for the copper (I) complex are higher than the burning rates for the copper (II) complex of the same parent compound.

(U) c. Analysis to Relate Subsurface Heating to Changes in Ammonium Perchlorate Crystal Structure

(C) An analysis to relate subsurface heating to changes in ammonium perchlorate crystal structure was conducted and is included as Appendix A to this report. It was concluded from this analysis that, if the concept of a constant surface temperature is valid and if the extrapolated value of thermal diffusivity is accurate to within 10 percent, the surface temperature of burning ammonium perchlorate is $440 \pm 30^{\circ}\text{C}$. In addition, calculations made using very high heat generation rates indicate that subsurface reactions are not an important factor in controlling the burning rate of ammonium perchlorate at pressures above 500 psi.

CONFIDENTIAL

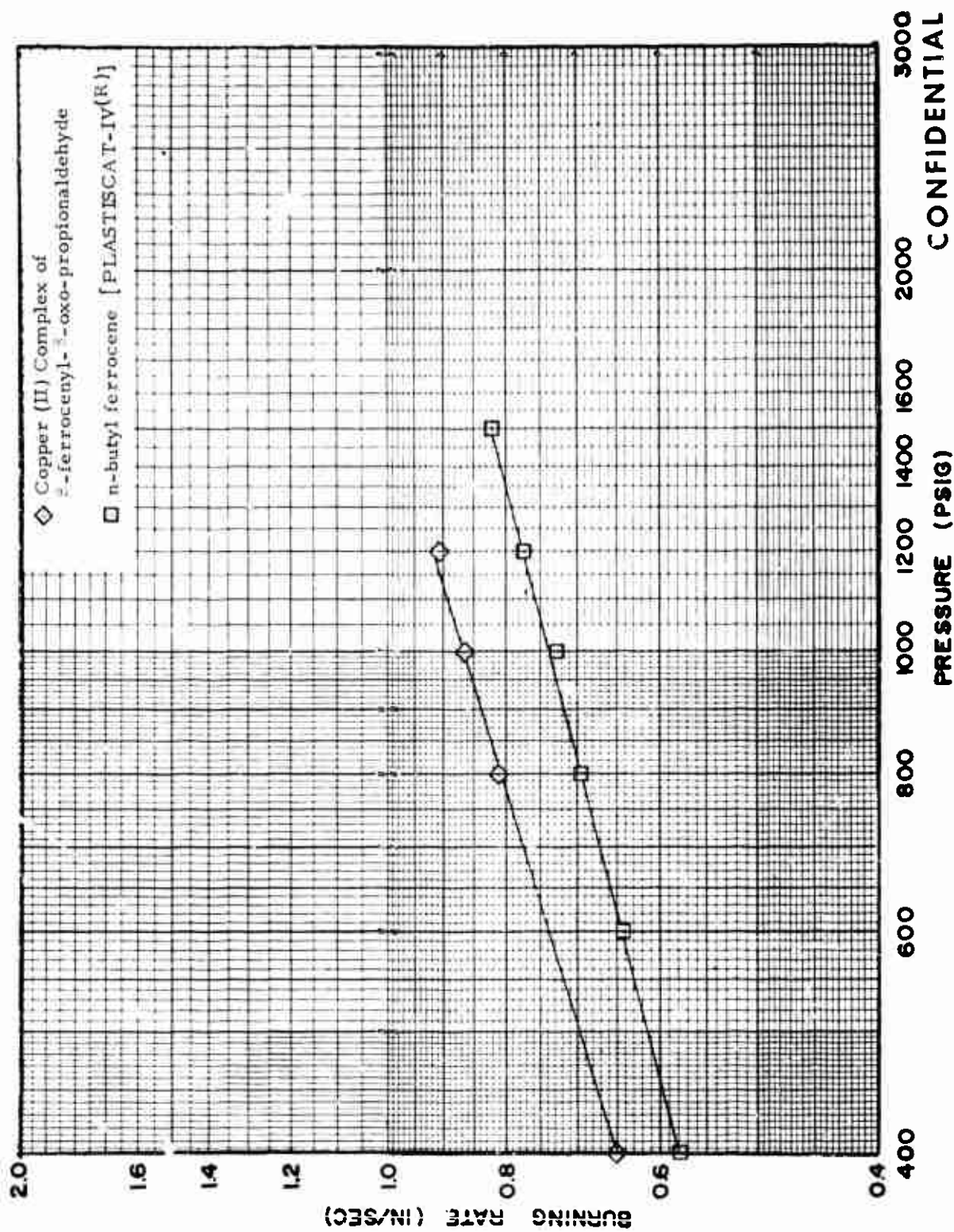


Figure 7. (C) Comparison of the Burning Rate of Propellant Catalyzed with PLASTISCAT - IV(R) and Copper (II) Complex of β -ferrocenyl- β -oxo-propionaldehyde.

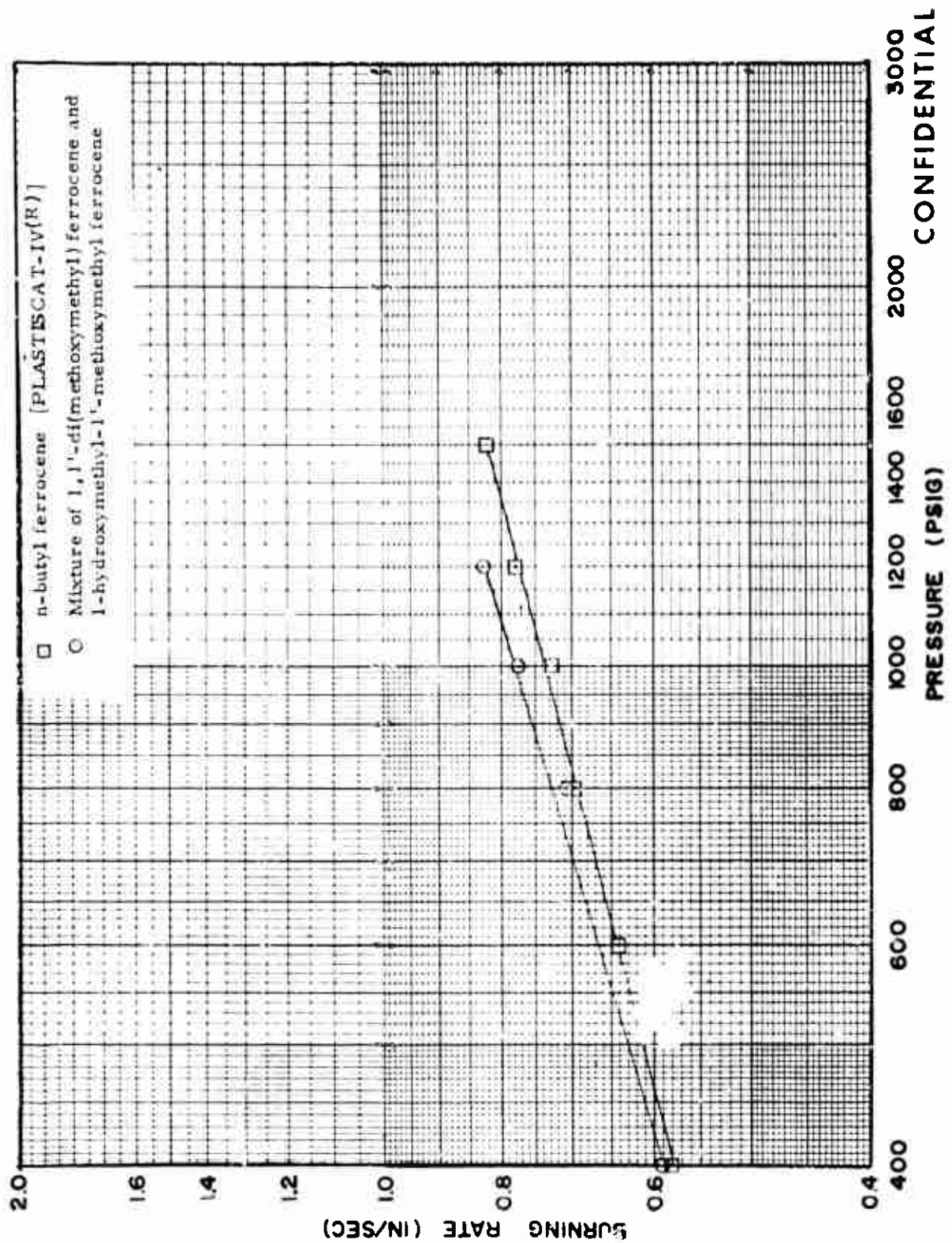


Figure 8. (C) Comparison of the Burning Rate Characteristics of Propellant Catalyzed with n-butyl ferrocene [PLASTISCAT-IV(R)] and a Mixture of 1,1'-di(methoxymethyl)ferrocene and 1'-methoxymethyl-1'-methoxymethyl ferrocene

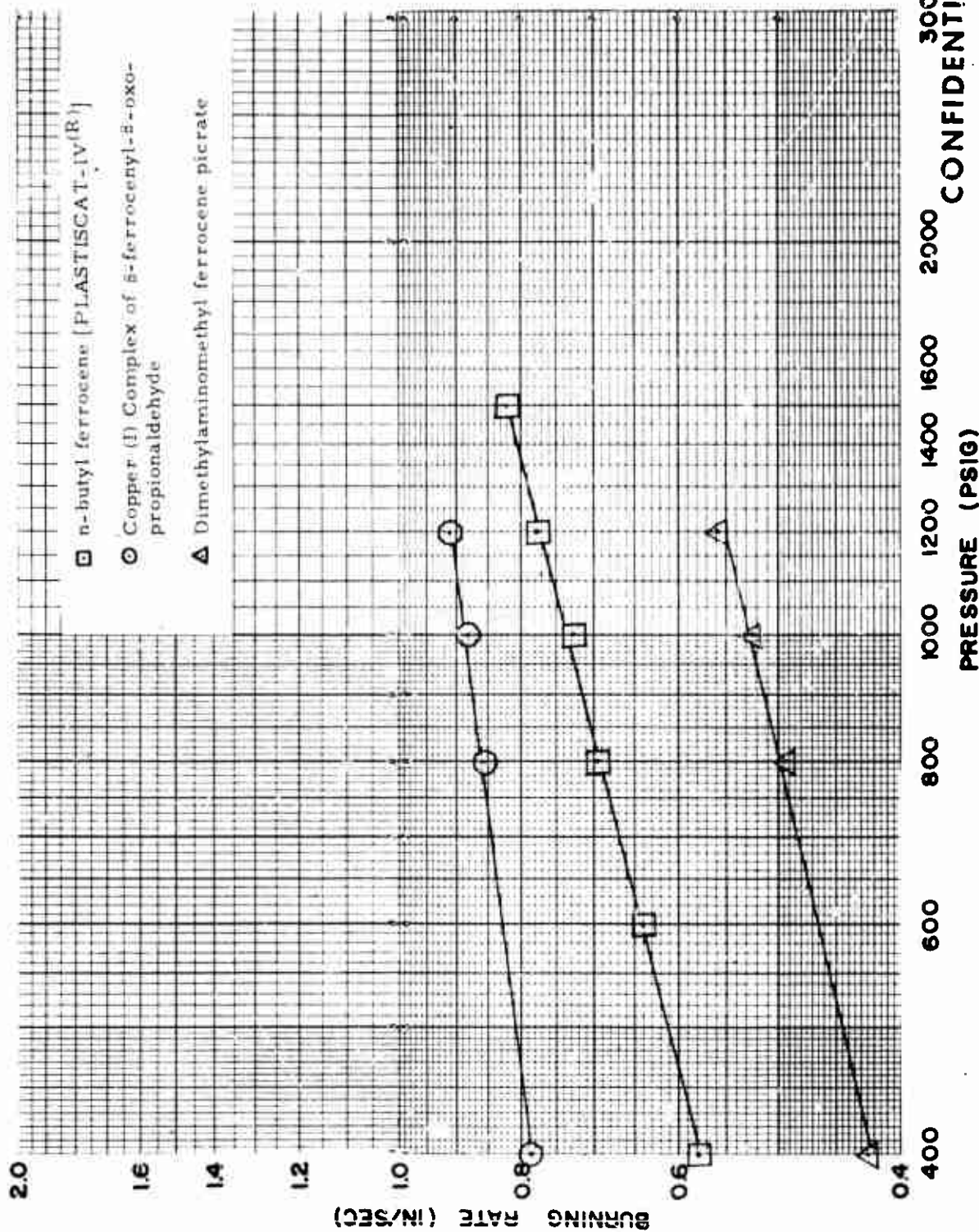


Figure 9. (C) Comparison of the Burning Rate of Propellant Catalyzed with PLASTISCAT-IV(R), Copper (I) complex of β -ferrocenyl- β -oxo-propionaldehyde, and Dimethyl aminomethyl ferrocenium Picrate.

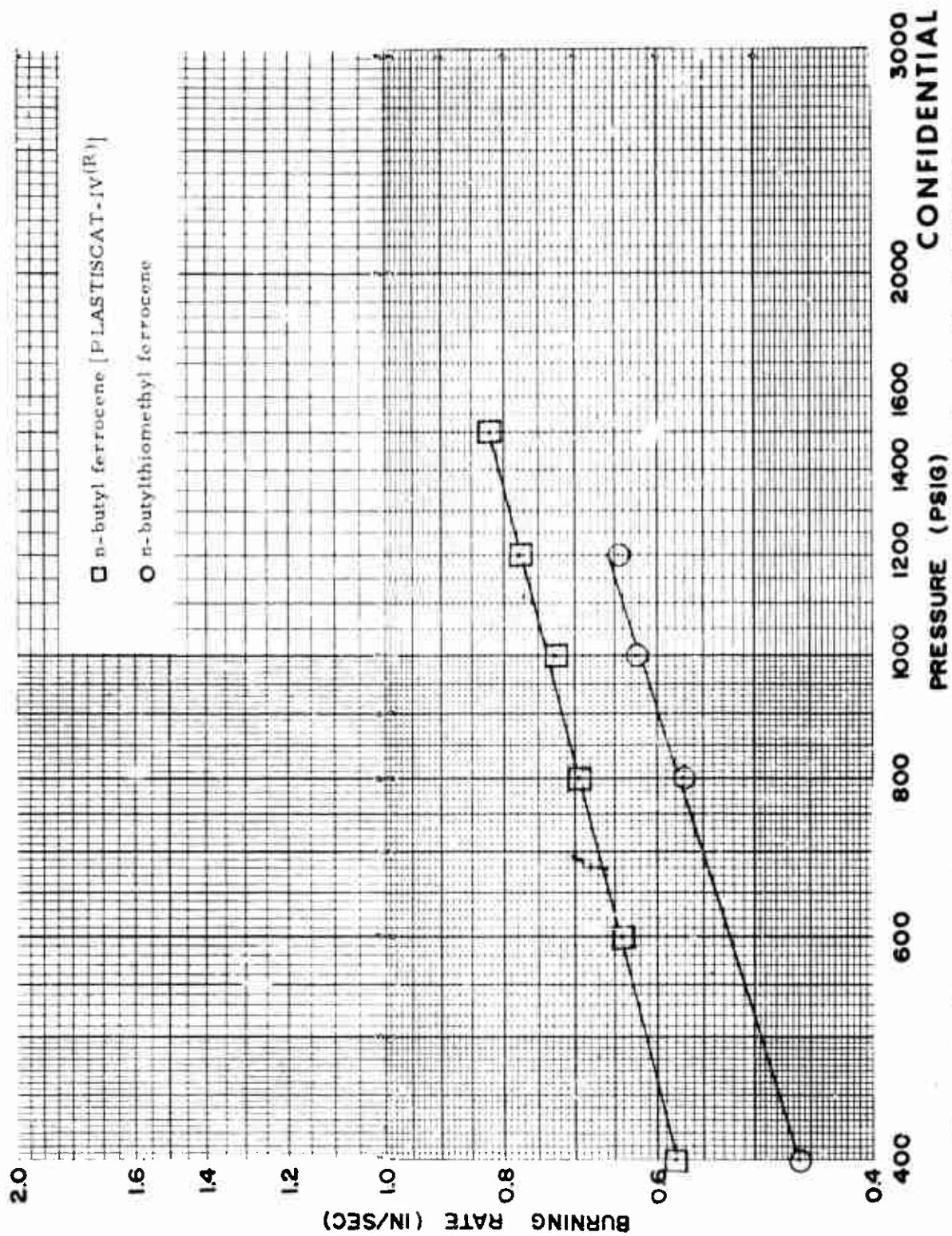


Figure 10. (C) Comparison of the Burning Rate of Propellant catalyzed with n-butyl ferrocene [PLASTISCAT-IV(R)] and n-butylthiomethyl ferrocene

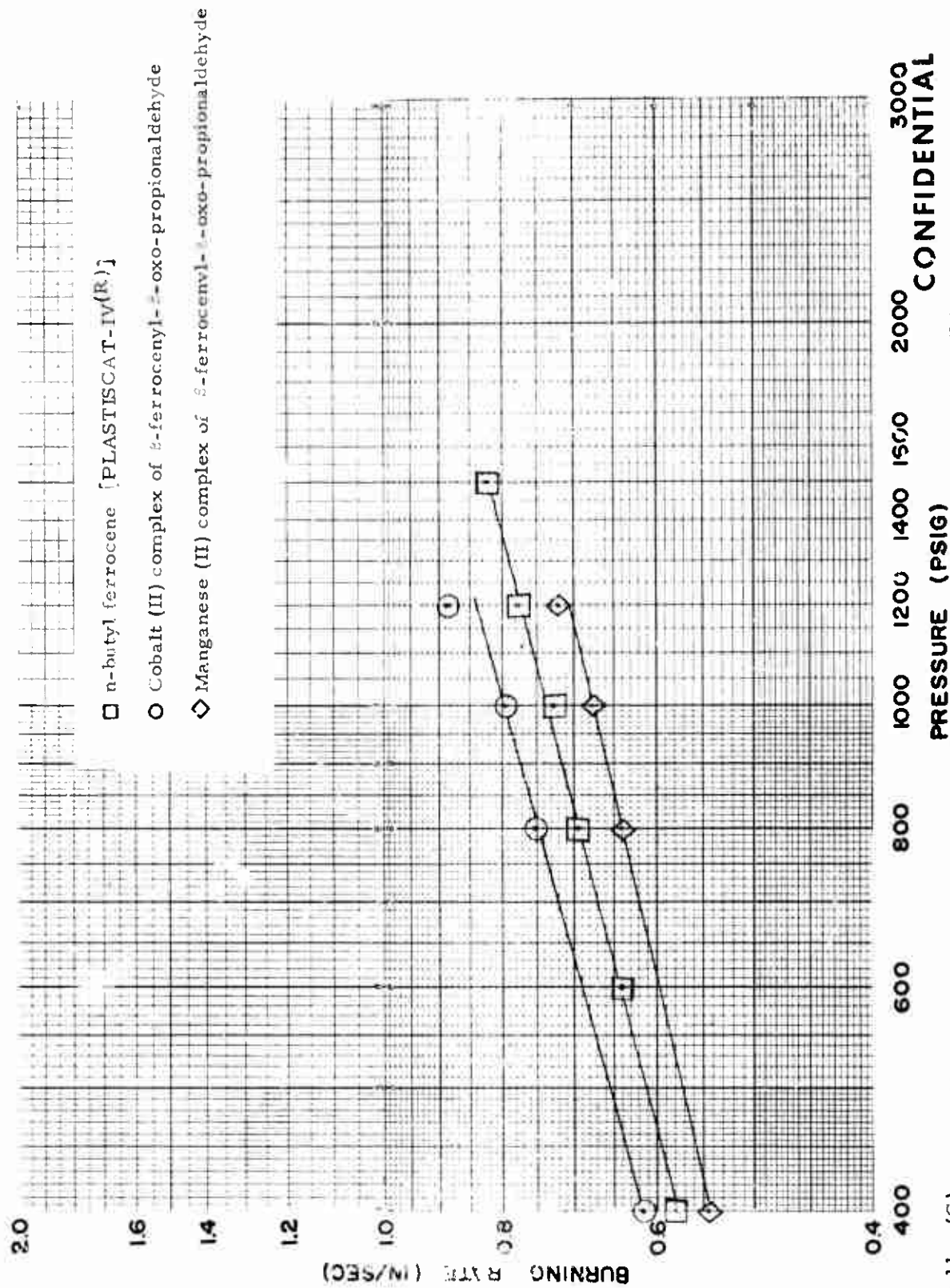


Figure 11. (C) Comparison of the Burning Rate of Propellant Catalyzed with PLASTISCAT-IV(R), Cobalt (III) complex of 3-ferrocenyl-β-oxo-propionaldehyde, and Manganese (II) complex of 3-ferrocenyl-β-oxo-propionaldehyde.

CONFIDENTIAL

SECTION III

CONCLUSIONS

(C) The following conclusions may be drawn from the work conducted during this reporting period:

Thermogravimetric analyses (TGA) of catalysts mixed with HC polymer showed that none of the compounds tested was effective in catalyzing the decomposition of HC polymer.

All of the catalysts tested appear to be compatible with HC polymer and MAPO at ambient temperature; however, under the 160°F conditions, only 2-methylthioethyl ferrocenylmethyl ether, 2-methoxyethyl ferrocenylmethyl ether, and dimethyl ferrocenylmethyl ammonium nitrate were compatible with both HC polymer and MAPO.

Propellants formulated with the copper (I) complex, the copper (II) complex and the cobalt (II) complex of β -ferrocenyl- β -oxo-propionaldehyde demonstrated burning rates higher than that of similar propellant containing n-butyl ferrocene [PLASTISCAT-IV^(R)] at the 2 percent level.

The burning rate of propellant formulated with the copper (I) complex was higher than the burning rate for the copper (II) complex of the same parent material.

The sulfur containing ferrocene derivatives synthesized were for the most part solids and were not effective as burn rate modifiers.

The salts of dimethylaminomethyl ferrocene do not contain enough iron to be effective solid burn rate catalysts at levels of 1 to 5 percent.

An analysis to relate subsurface heating to changes in ammonium perchlorate crystal structure was conducted. It was concluded from this analysis that, if the concept of a constant surface temperature is valid and if the extrapolated value of thermal diffusivity is accurate to within 10 percent, the surface temperature of burning ammonium perchlorate is $440 \pm 30^\circ\text{C}$. In addition, calculations made using high heat generation rates indicate that subsurface reactions are not an important factor in controlling the burning rate of ammonium perchlorate at pressures above 500 psi.

CONFIDENTIAL

PRECEDING PAGE BLANK NOT FILMED

UNCLASSIFIED

APPENDIX A

(Unclassified)

ANALYSIS TO RELATE SUBSURFACE HEATING TO CHANGES
IN AMMONIUM PERCHLORATE CRYSTAL STRUCTURE

UNCLASSIFIED

UNCLASSIFIED

APPENDIX A

(Unclassified)

ANALYSIS TO RELATE SUBSURFACE HEATING TO CHANGES
IN AMMONIUM PERCHLORATE CRYSTAL STRUCTURE(U) 1. Introduction

(U) An analysis was conducted to relate surface temperature, subsurface reactions, and crystal structure of burning ammonium perchlorate (AP) using a more complete mathematical model to analyze further the data presented in a series of papers by Beckstead, Hightower, and Price¹⁻³. The results of this analysis have direct application to the development and application of burning rate models to explain observed propellant phenomena. Since the burning rate of heterogeneous propellants containing AP is controlled by the AP particle size and percentage, it is not sufficient to treat propellant burning in the mean but rather the burning of individual ingredients must be considered. To account accurately for the heat transferred to the burning AP surface, the contribution of subsurface heating and the value of surface temperature must be known. Since AP decomposes at above 250°C and the surface temperature of burning composite propellants containing AP is above 400°C, considerable difficulty is being encountered in measuring its thermophysical characteristics in the temperature range where the burning rate controlling reactions occur, i.e., above 250°C. Several carefully controlled optical measurements^{4,5} and embedded micro-thermocouple measurements^{6,7} of surface temperature have been conducted. These experimental techniques were recently reviewed by Friedman⁸. In general, the optical techniques are not effective at rocket motor operating pressures and micro-thermocouples are too large to follow the temperature rises in the propellant ingredients. In addition, since the propellant is a heterogeneous substance, difficulty is encountered in discriminating between mean and local effects.

(U) The basis of this analysis is the establishment of the heat balance to correlate experimental observations of the crystallographic phase transition from an orthorhombic to a cubic structure in burning AP crystals.

(U) 2. Background

(U) Several investigators have recognized that since the crystalline transformation from orthorhombic to cubic occurs approximately midway between the ambient propellant temperature and the burning surface temperature, it could be used to deduce surface temperatures of burning propellants.

UNCLASSIFIED

McGurk⁹ examined optically very thin microtomed sections of AP composite propellants before and after extinguishment. He noted an optical discontinuity below the extinguished surface of individual AP particles which he postulated to be the interface between the orthorhombic and cubic phases prior to propellant extinguishment. Of course, after extinguishment, the cubic structure reverts back to the orthorhombic structure. In addition, McGurk suggested that the 100°C isotherm could be bracketed by examining the effect of surface heating on voids containing a saturated water and ammonium perchlorate solution. However, McGurk did not make quantitative determinations of surface temperature.

(U) Selzer¹⁰ photographed thin slices of burning composite propellant and established the cubic phase thickness of AP from patterns produced by polarized light. Although Selzer's technique produced a wealth of data, his attempt to deduce a value of surface temperature was premature because of experimental and analytical difficulties. Since his optics were penetrating a relatively thick section of propellant, he was not measuring the cubic phase thickness at a discrete point. In addition, as pointed out by Beckstead and Hightower², Selzer's analytical treatment to deduce surface temperature was not sufficiently comprehensive.

(U) Because of the transient nature of the burning of individual AP particles, it is doubtful the data of McGurk and Selzer can be used to make accurate determinations of the heat balance that occurs in the solid phase. As part of the work¹¹ being conducted to develop a more comprehensive burning rate model, equations were solved that approximate the transient two-dimensional (the third dimension is accounted for by spherical symmetry) heat conduction that occurs as individual AP particles are consumed. Figure 1 shows analytical results for three spherical AP particles being burned at 700 psi. Similar transients have been observed in micro-window bomb photographs. The calculations reveal that because the AP particles are preheated as the adjacent binder layer is consumed, a burning rate overshoot occurs. This initial overshoot decays as the preheated portion of the AP is consumed. As the spherical AP particle burns, the ratio of exposed surface to immediate subsurface volume continuously varies. This coupled with the normal induction time to establish thermal profiles results in continuously varying burning rates. Just prior to the burnout of the AP particle, heat is transferred to the binder layer that separates adjacent AP particles. Since binder has a thermal conductivity approximately 50% lower than the thermal conductivity of AP, more heat is retained in the AP crystal causing the rapid increase in burning rate.

(U) The excellent experiments recently reported by Beckstead and Hightower eliminated many of the shortcomings of the previous studies. They burned very pure, single AP crystals in a nitrogen atmosphere. The crystals were quenched by rapid depressurization. The cubic phase thickness was established by examining many cleaved crystals under polarized light (Figure 2).

UNCLASSIFIED

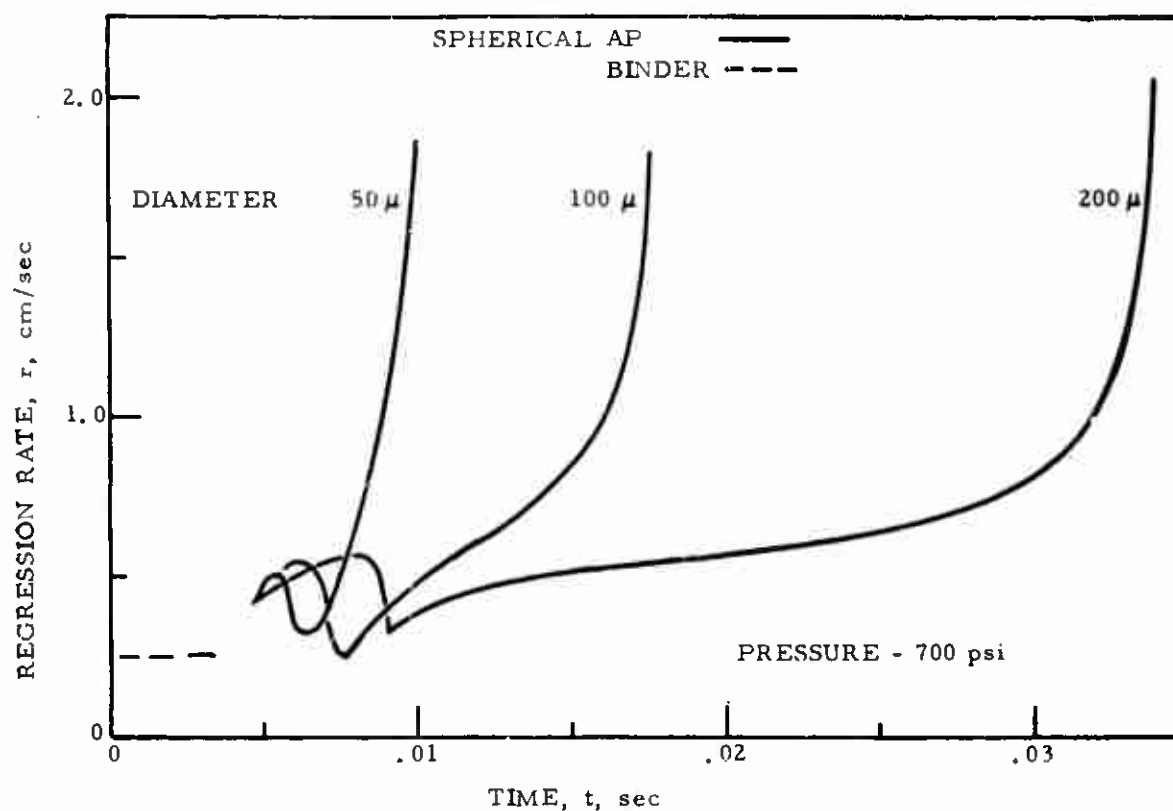


FIGURE A-1. BURNING TRANSIENTS OF SPHERICAL AMMONIUM PERCHLORATE WITH PARTICLE DIAMETER AS A PARAMETER

UNCLASSIFIED

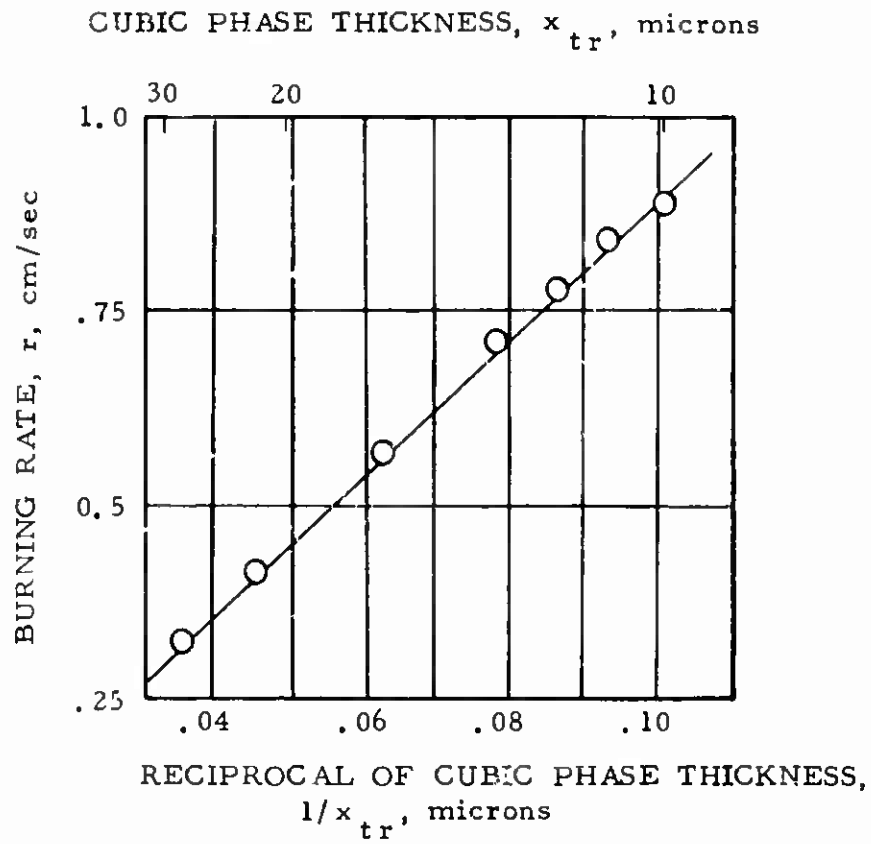


FIGURE A-2. THE PHASE TRANSITION THICKNESS AS A FUNCTION OF BURNING RATE AS MEASURED BY BECKSTEAD AND HIGHTOWER²

A very important conclusion was that the product of AP burning rate, r , times cubic phase thickness, x_{tr} , was nearly constant. In addition, the circles on Figure 2 are indicative of the variations in measuring a large number of samples¹², hence the scatter observed by Selzer did not occur in the single crystal experiments. Beckstead and Hightower² solved a boundary value problem for the heat balance at the cubic-orthorhombic interface and arrived at the important conclusion that the temperature of the solid phase surface is nearly constant. They postulated that the higher surface temperatures measured optically⁵ were measurements of the surface of a liquid layer which Hightower had previously reported to exist¹³.

(U) 3. Analysis

(U) As shown on Figure 3, the decomposition of a burning AP crystal can be considered to occur in several phases: 1) relatively gradual heating of the orthorhombic phase ($<10^4$ °C/sec for $r = 0.8$ cm/sec), 2) transition from orthorhombic structure to cubic structure, 3) relatively rapid heating of the cubic phase ($>10^5$ °C/sec), 4) the possible formation of a liquid layer, 5) sublimation or gasification to AP vapors, and 6) gas phase decomposition of AP vapors. Since for steady-state conditions the surface of the solid phase is regressing at a rate equal to the propagation rate of the transition zone, the thickness of the cubic phase, x_{tr} , is constant. The transition from cubic to orthorhombic is an endothermic process which requires 19.5 cal/gram at slow heating rates (less than 100 °C per minute). Since this heating rate is very much less than the 10^4 °C/sec that occurs during normal propellant burning, it is not entirely certain that the same endothermic reaction occurs in a propellant burning at pressures above 500 psi. Indeed, one of the stated objectives of this analysis is to evaluate the extent to which AP subsurface reactions are a factor in controlling propellant burning rate. By selecting the AP solid phase boundary as a reference point, the effect of the postulated liquid phase is not a factor in this analysis.

(U) While the relative effects can be studied using approximate values for the thermal properties, the objective of this analysis is to obtain quantitative results by taking full advantage of the best available thermal property determinations. Since orthorhombic phase thermal properties are relatively well established compared to those of the cubic phase, the thermal property discussion will be limited to the cubic phase. The cubic phase density of 1.76 gm/cc calculated by Markowitz¹⁴ was selected. However, hot stage photographs of single AP crystals above 260 °C taken by Flanigan have shown that the crystal growth does not support the change in density predicted by Markowitz. The specific heat values were taken from the JANAF data¹⁴. The discontinuity in specific heat that occurs at 243 °C is consistent with the predicted change in density. The orthorhombic phase thermal conductivity of Rosser, Inami, and Wisel¹⁶ provides a basis for determining thermal

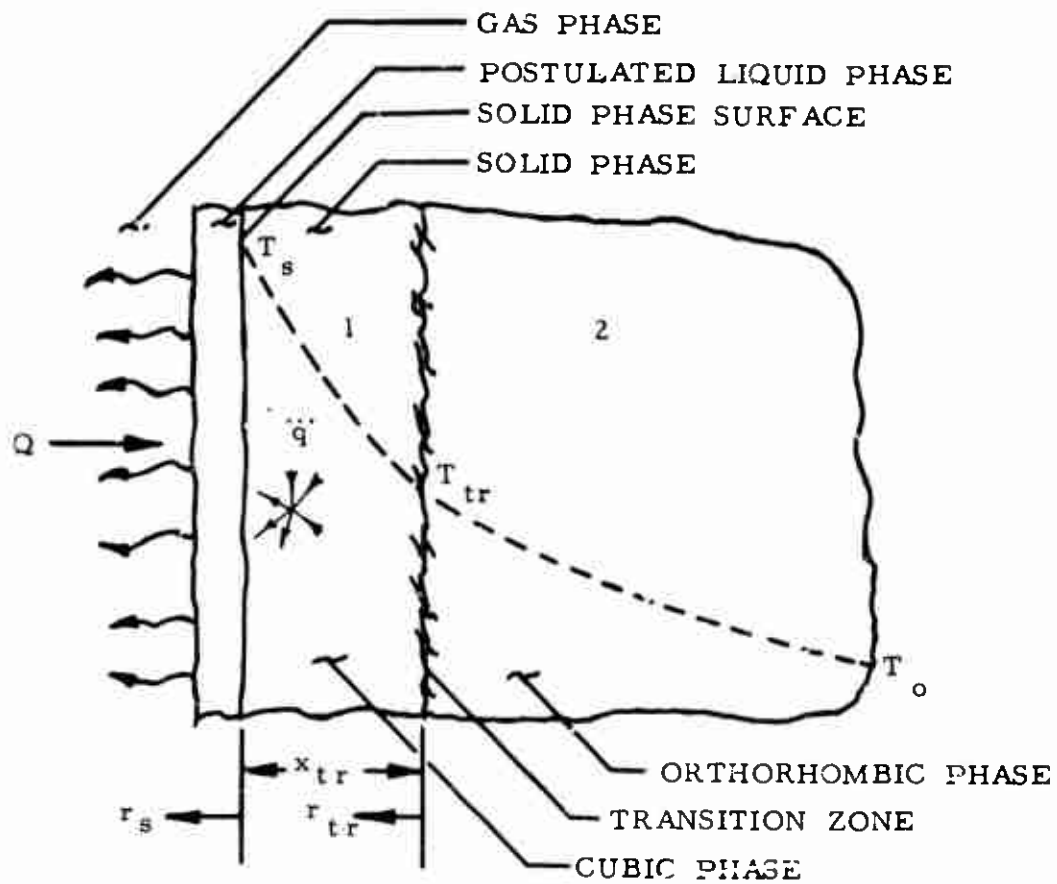


FIGURE A-3. PHYSICAL SITUATION CONSIDERED BY MATHEMATICAL SOLUTION

conductivity of the cubic phase by extrapolation. The problem is to decide how to extrapolate the data to the cubic phase. The data points on Figures 4 and 5 are Rosser's data corrected for porosity in the manner suggested in Reference 16. Beckstead and Hightower² consider the data point at 215°C to be suspect. If it is ignored, the data can be correlated as a function of reciprocal absolute temperature. The thermal conductivities of other crystals have been correlated over a wide range of temperatures using reciprocal temperature. Thus, by extrapolating the data a value of thermal conductivity at 400°C of 0.00084 cal/sec-cm-°C is obtained from the linear correlation (Figure 4) and a value of 0.00097 cal/sec-cm-°C is obtained from the reciprocal temperature correlation (Figure 5). A -10% error in cubic phase thermal conductivity will increase calculated surface temperature by approximately 30°C. The arguments put forth by Beckstead and Hightower for extrapolation based on reciprocal temperature appear reasonable and will be adopted for this analysis.

(U) a. Conduction in Ammonium Perchlorate

(U) Using the physical situation described above, the equations governing conduction within a moving homogeneous, isotropic, reacting medium is

$$\rho c \partial T / \partial t = \partial [k (\partial T / \partial x)] / \partial x + r \partial T / \partial x + \ddot{q} \quad (1)$$

The sign convention for burning AP is: burning rate, r , and latent heat of crystallographic phase transition (for endothermic reaction), λ , less than zero. During steady-state burning of the AP crystal the boundary conditions are:

$$\begin{aligned} \text{At } x = x_{tr}: \quad T &= T_{tr} \\ -k_1 \quad dT/dx &= [-k_2 \quad dT/dx] = r \rho_2 \lambda \end{aligned} \quad (2)$$

After extinguishment the boundary conditions become:

$$\begin{aligned} \text{At } x = 0: \quad T &< T_s \\ \text{At } x = x_{tr}: \quad T &= T_{tr}, \quad r \neq 0 \\ T &< T_{tr}, \quad r = 0 \end{aligned}$$

The above equations were solved using explicit finite difference techniques. Because of the very small time and distance increments that were used, considerable attention had to be given to developing an efficient computational procedure. The steady-state profiles were established by relaxation;

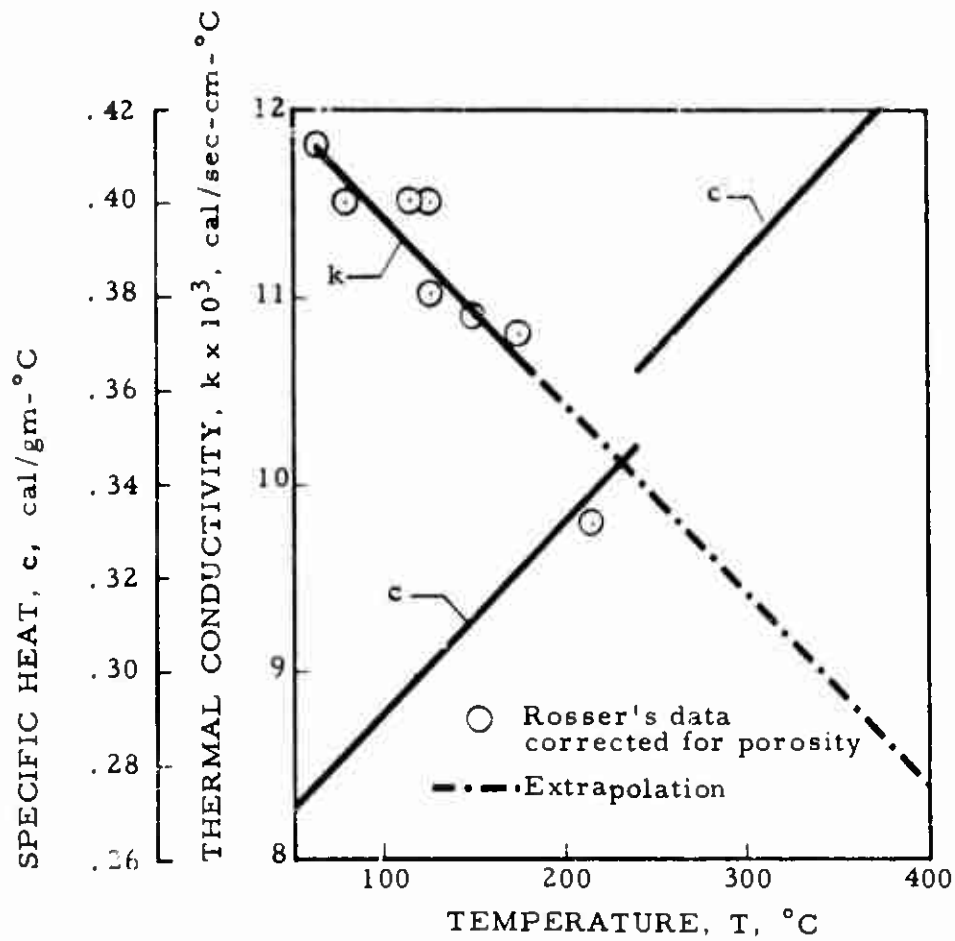


FIGURE A-4. THERMAL CONDUCTIVITY AND SPECIFIC HEAT OF AMMONIUM PERCHLORATE

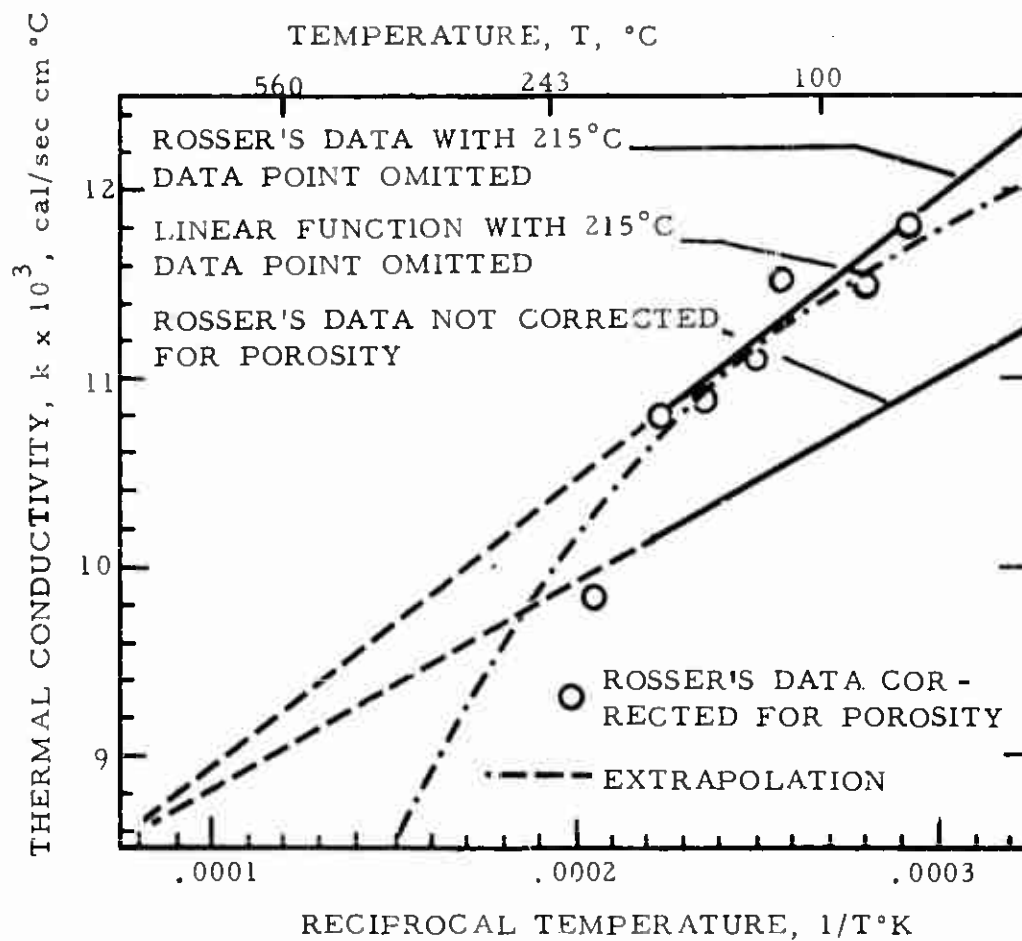


FIGURE A-5. RELATIONSHIP BETWEEN THERMAL CONDUCTIVITY AND TEMPERATURE

the temperature time history after extinguishment was calculated using a forward integration.

(U) b. Steady-State Closed Form Solutions

(U) Assuming steady-state conditions, constant thermal properties, and no heat generation, Equation 1 reduces to

$$0 = (k/\rho c) (d^2 T/dx^2) + r T/\partial x \quad (3)$$

Solving Equation 3 with the steady-state boundary conditions, yields

$$T_s = T_{tr} + [\exp(-rx_{tr}/\alpha_1) - 1] [(\rho_2 c_2 / \rho_1 c_1) T_{tr} - (\rho_2 c_2 / \rho_1 c_1) T_0 - \rho_2 \lambda / \rho_1 c_1] \quad (4)$$

This equation differs from the equation reported by Beckstead and Hightower² because of the manner in which they considered the boundary condition at the cubic-orthorhombic interface. They wrote boundary condition corresponding to Equation 3 as

$$-k_1 dT/dx = [-k_2 dT/dx] + r T_{tr} (\rho_2 c_2 - \rho_1 c_1) = r \rho_2 \lambda \quad (5)$$

The last term on the left hand side of the equation was included to account for the change in heat content across the cubic-orthorhombic interface. This term is considered to be redundant because the effect is accounted for in the value of latent heat, λ . The equation for steady-state condition derived by Beckstead and Hightower is

$$T_s = T_{tr} + [\exp(-rx_{tr}/\alpha_1) - 1] [T_{tr} - (\rho_2 c_2 / \rho_1 c_1) T_0 - \rho_2 \lambda / \rho_1 c_1] \quad (6)$$

(U) c. Effect of Physical Property Accuracy

(U) To evaluate the effect of physical property accuracy on calculated surface temperature, the variables in Equation 4 were perturbed. The results of Figure 6 were obtained using the indicated properties to define the datum case. The results indicate that the property which is least understood, the cubic

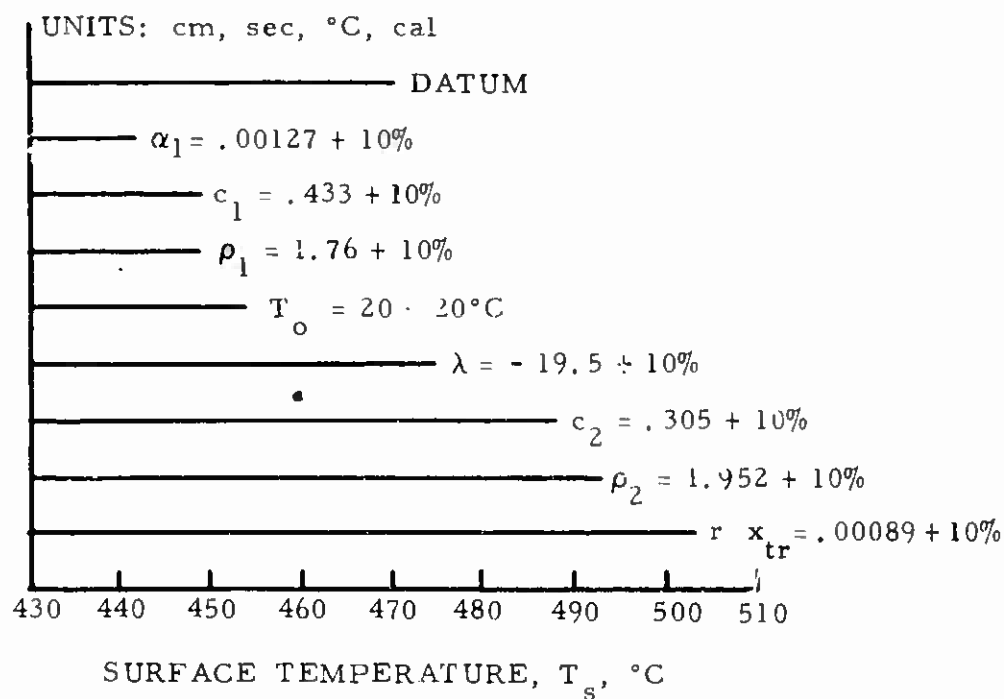


FIGURE A-6. EFFECT OF PHYSICAL PROPERTY ACCURACY ON SURFACE TEMPERATURE

phase thermal diffusivity, has the greatest effect on the accuracy of the calculated surface temperature value. In addition, the values of c_1 and ρ_1 are also uncertain. Since c_1 and ρ_1 are always used as a product, $\rho_1 c_1$, it is felt that the value of the product is known to within 5%. The accuracy of the other physical property values used in the equation are well known relative to the accuracy of α_1 .

(U) 3. Results

(U) A series of numerical computations were performed in which the values of the solid phase surface temperature and burning rate were varied. The first calculations considered that the only subsurface reaction was during the transition from orthorhombic to cubic crystal structure; the thermal physical properties of Figure 5 were used. Figure 7 indicates the relative importance of the transients after strand extinguishment. For a surface regression of 0.6 cm/sec, for the lower value of surface temperature (410°C) approximately 0.5 millisecond is required for the regression of the cubic layer to stop. For the higher surface temperature, 460°C, approximately 0.7 millisecond is required. As the regression rate increases from 0.6 cm/sec to 1.2 cm/sec, the increase in the cubic phase thickness that occurs after extinguishment varies from 11 to 10%, respectively.

(U) Figure 8 shows the effect of surface temperature on the thickness of the cubic phase. When the surface temperature is related to the measured cubic phase thickness, a value of 470°C is obtained if the transients after extinguishment are ignored. However, if the measured cubic phase thickness is related to the predicted cubic phase thickness after cooldown, a decreased predicted surface temperature of 442°C is obtained.

(U) The difference between the exact and numerical solution for the steady-state condition is less than 1%. Using the variable thermal properties of Figures 4 and 5 results in slightly higher values for the steady-state cubic phase thickness and the same value for the cubic phase thickness after cooldown (Figure 8). This agreement is expected because for steady-state the net heat balance can be accounted for exactly by the mean thermal properties; and for the transient condition the variation in temperature is small enough that the properties evaluated at mean temperatures accurately represent the heat balance.

(U) Figure 9 shows cubic phase thickness over a range of burning rates. The circles are deduced values of surface temperature based on the measured cubic phase thicknesses.

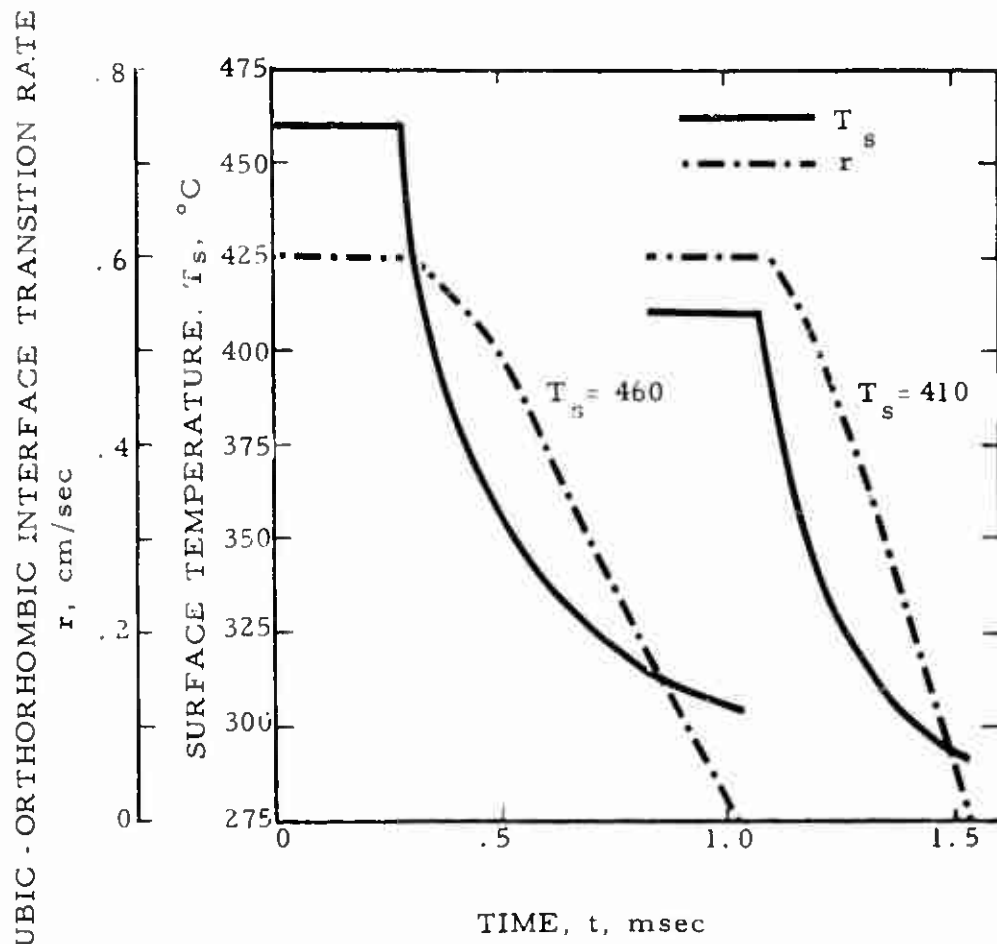


FIGURE A-7. TRANSIENTS AFTER EXTINGUISHMENT

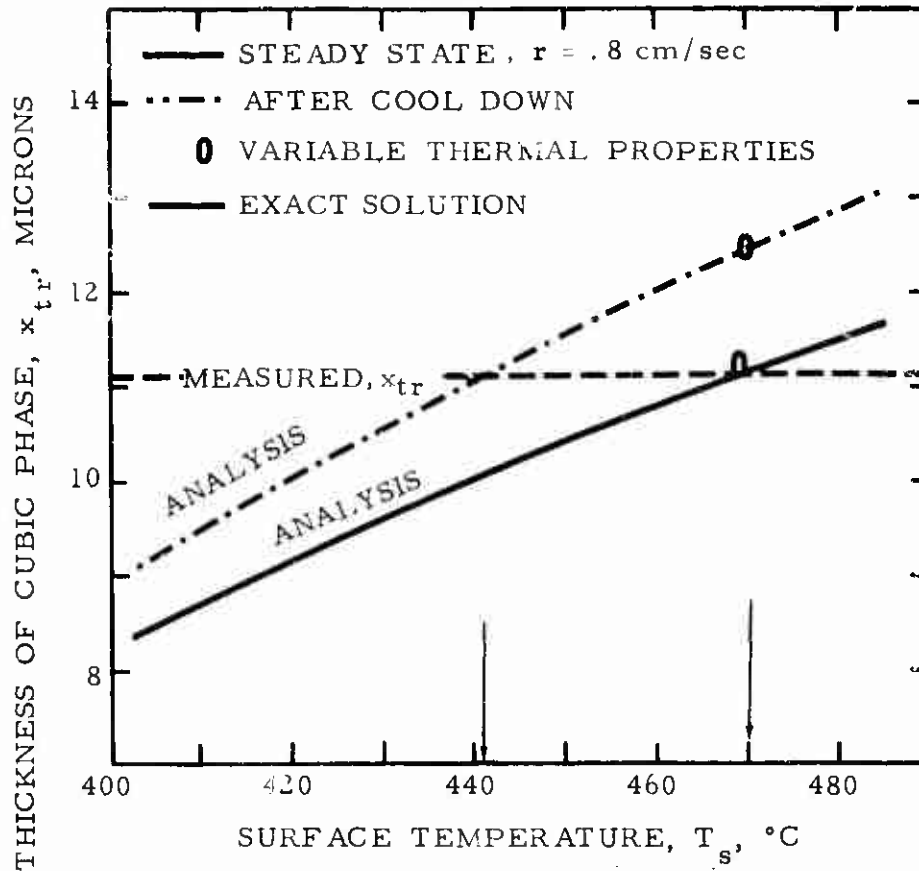


FIGURE A-8. CUBIC PHASE THICKNESS AS A FUNCTION OF SURFACE TEMPERATURE

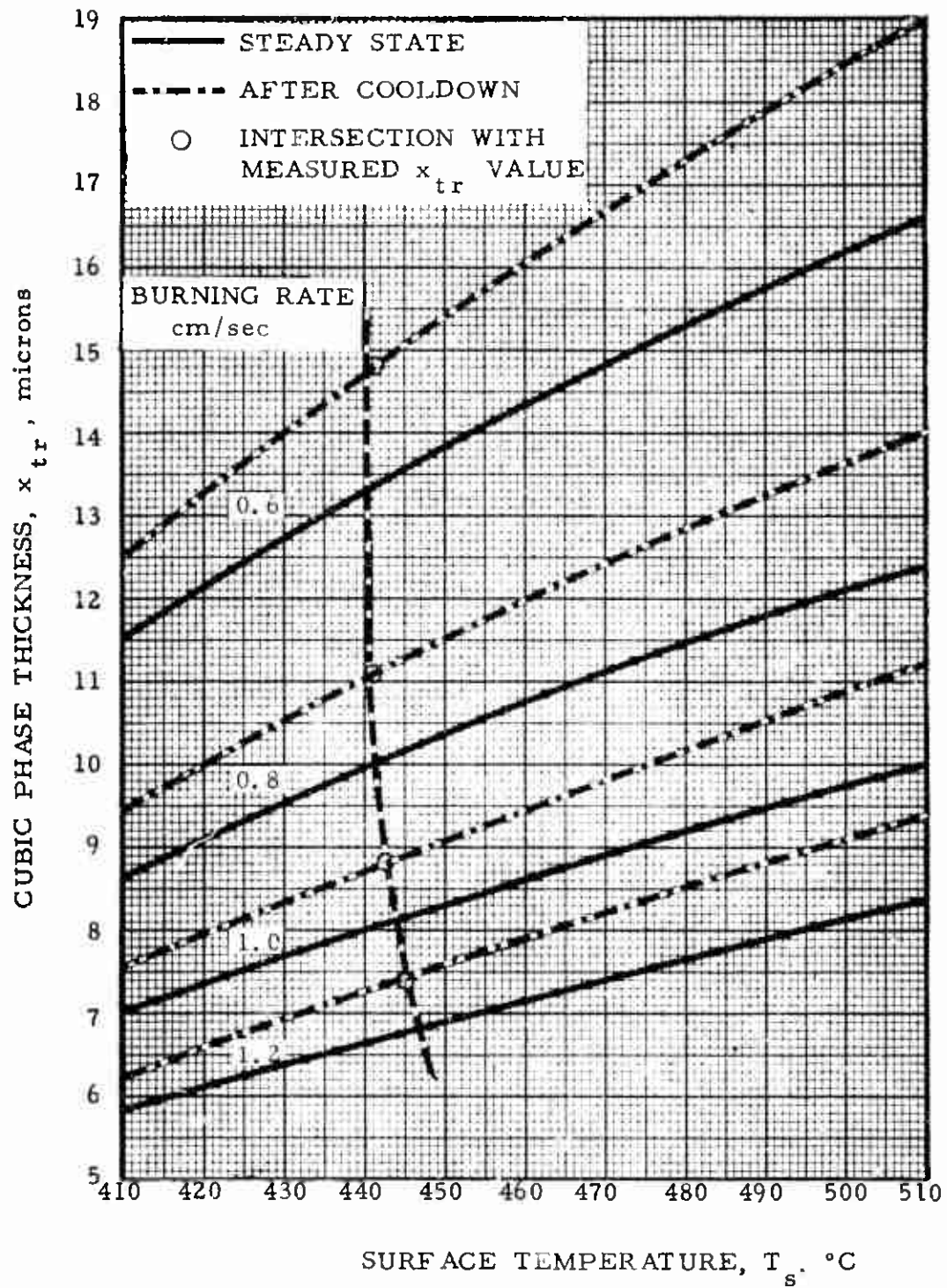


FIGURE A-9. CUBIC PHASE THICKNESS AND SURFACE TEMPERATURE OVER A RANGE OF SURFACE TEMPERATURE

(U) a. Subsurface Reactions

(U) Figure 10 is a cross-plot of the surface temperatures of Figure 8 and shows that surface temperature increases slightly with increasing burning rate. The slight increase in T_s provides a basis for discussing the relative effects of subsurface reactions. It will be assumed that the surface temperature of the solid phase is constant and that the increase in calculated surface temperature with increasing rate can be explained by the experimental error in the measurement of x_{tr} . The assumption of a constant surface temperature is not inconsistent with data in light of the observations made by Beckstead and Hightower² that surface temperatures measured optically is the surface temperatures at the surface of a liquid phase.

(U) Two conditions may be considered: 1) a net subsurface endothermic reaction, and 2) a net subsurface exothermic reaction. By net reaction the latent heat of phase change between the orthorhombic and cubic crystal structure is included with any subsurface reaction that may occur in the cubic phase. Figure 11a shows that diminishing the net endothermic reaction (or regression toward a greater exothermic reaction) the actual surface temperature will decrease. Also if there were a subsurface reaction, its fraction of depletion would tend to diminish with increasing rate as indicated in Figure 11b.

(U) Now we will consider the situation: 1) during the actual burning of AP there is a net solid phase endothermic reaction, and it is ignored in the calculations, and 2) the measured values of x_{tr} were used to deduce surface temperature. The trends shown in Figures 11a and 11b indicate that as a result of the above situation, the error in the deduced value of surface temperature would be in the direction shown on Figure 10. If a similar argument is attempted for a net exothermic reaction, the reverse trend of that indicated by Figure 10 is required. Thus, the surface temperature variations of Figure 10 are not great enough to conclusively support a net endotherm, they certainly do not support the existence of an exothermic reaction. In any event, the subsurface reaction is not a primary effect, for, if it were, greater discrepancy in calculated (or deduced) values of surface temperature would occur.

(U) The calculations of the cubic phase thickness were repeated with the subsurface heat generation expressed by the first order reaction equation

$$\ddot{q}_i = Z Q f(t) \exp(-E/RT)$$

The heat evolution in the solid phase was assumed to be 200 cal/gm and the value of the frequency factor was varied from 10^{16} to 10^{18} . Z equal to 10^{18} is considerably above the highest values¹⁷ that have been assigned to it. Even for the high values of frequency factor, less than 1% change in surface temperature was calculated. While using these external assumptions, a

UNCLASSIFIED

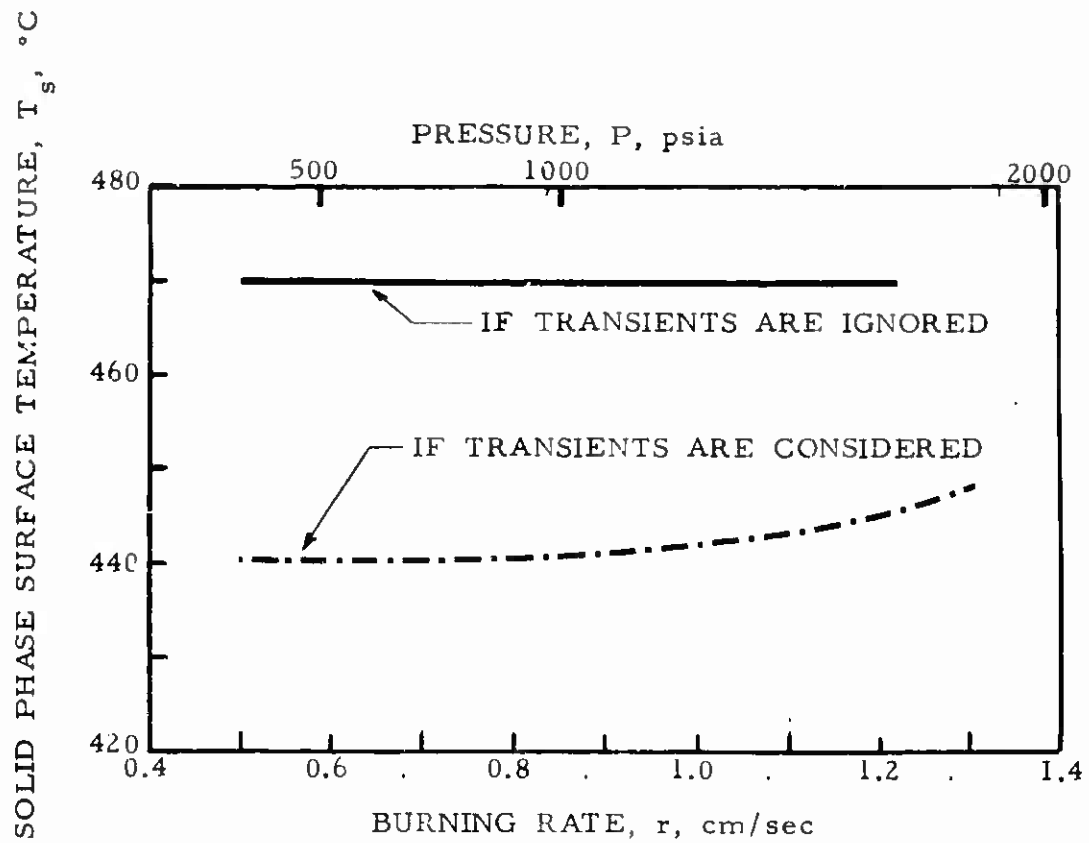
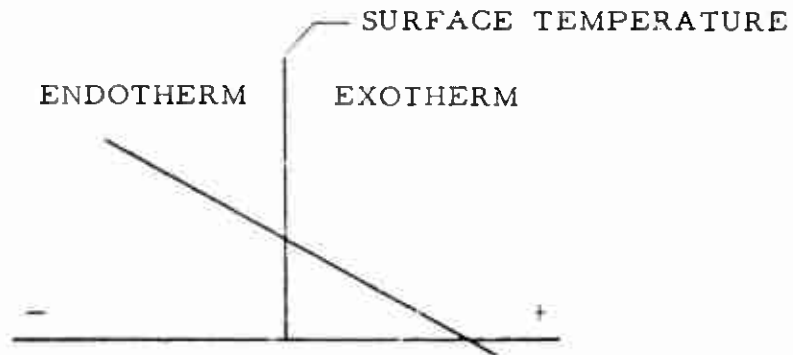
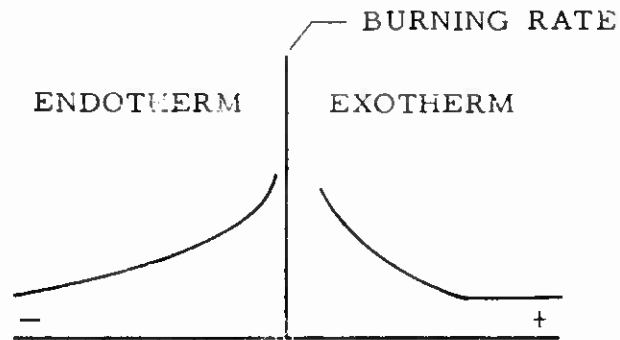


FIGURE A-10. DEDUCED VALUE OF SURFACE TEMPERATURE WHEN LATENT HEAT OF ORTHORHOMBIC TO CUBIC PHASE CHANGE IS THE ONLY SUBSURFACE REACTION

UNCLASSIFIED



A. HEAT EVOLUTION ACCOMPANYING CHEMICAL OR PHYSICAL CHANGE IN SOLID PHASE



B. HEAT EVOLUTION ACCOMPANYING CHEMICAL OR PHYSICAL CHANGE IN SOLID PHASE

FIGURE A-11. RELATIONSHIP BETWEEN SURFACE TEMPERATURE, BURNING RATE, AND HEAT EVOLUTION

CONFIDENTIAL

subsurface heat release within the first two microns was calculated; the heat release was not of sufficient magnitude to affect burning rate. Again, these calculations confirm that even though the solid phase temperatures are of the proper magnitude for subsurface reactions to occur, the stay time is too short for the reaction to the extent that it affects burning rate.

(U) On the basis of kinetic data obtained at very low heating rates (less than $100^{\circ}\text{C}/\text{min}$) Feinauer, Waesche, and Wenograd¹⁷ have postulated that the condensed phase reactions play an important role in the control of composite solid propellant burning rates. The results of this analysis conclusively demonstrate that since the time available for subsurface reactions to occur in practical propellants is several orders of magnitude less than the heating periods used in the laboratory apparatus employed to obtain the kinetic data, the condensed phase reactions are not of sufficient magnitude to control propellant burning rate.

(U) 4. Conclusions

(C) If the concept of a constant surface temperature is valid and if the extrapolated value of thermal diffusivity is accurate to within 10%, the surface temperature of burning AP is $440 \pm 30^{\circ}\text{C}$. In addition, calculations made using very high heat generation rates indicate that subsurface reactions are not an important factor in controlling the burning rate of AP at pressures above 500 psi.

CONFIDENTIAL

CONFIDENTIAL

REFERENCES

1. Hightower, J. D. and Price, E. W., "Experimental Studies of the Combustion Zone of Composite Propellants," ICRPG /AIAA Solid Propulsion Conference (July 1966).
2. Beckstead, M. W. and Hightower, J. D., "On the Surface Temperature of Deflagration Ammonium Perchlorate Crystals," AIAA Paper, No. 67-68, presented at 5th Aerospace Sciences Meeting, New York, N. Y., (January 23-26, 1967).
3. Hightower, J. D. and Price, E. W., "Combustion of Ammonium Perchlorate," presented at the 11th Symposium (International) on Combustion, Berkeley, California (August 1966).
4. Powling, J. and Smith, W. A. W., "The Surface Temperature of Burning Ammonium Perchlorate," Combustion and Flame 7, 269-277 (1963). Also *ibid* 6, 173, 1962.
5. Powling, J. and Smith, W. A. W., "The Surface Temperature of Ammonium Perchlorate Burning at Elevated Pressures," 10th Symposium (International) on Combustion (The Combustion Institute, Pittsburgh, Pa., 1965).
6. Bobolev, V. K., Glazkova, A. P., Zenin, A. A., and Leipunskii, O. I. "Temperature Distribution in Ammonium Perchlorate When Burning," Dokl. Akad. Nauk, 151, (3), 604-607, 1963, U.S.S.R., Translated by Technical Information and Library Services, Ministry of Aviation, Nottingham, Great Britain, TIL/T.5475, N64-18141, (Issued January 1964).
7. Sabadell, A. J., Wenograd, J., and Summerfield, M., "The Measurement of the Temperature Profiles of Solid Propellants by Microthermocouples," Princeton University, Aeronautical Engr. Dept. 664 (1963).
8. Friedman, Raymond, "Experimental Techniques for Solid Propellant Combustion Research," AIAA Paper 67-67, presented at Fifth Aerospace Sciences Meeting, (January 1967).
9. McGurk, J. L., "Microscopic Determination of Propellant Combustion Surface Temperatures," Proceedings of 1st ICRPG Combustion Instability Conference, CPIA Publication 68, 345-59, (January 1965).

UNCLASSIFIED

10. Selzer, H. , "The Temperature Profile Beneath the Burning Surface of an AP-Composite Propellant," presented at the 11th Symposium (International) on Combustion, Berkeley, California (August 1966).
11. Caveny, L. H. , "Subsurface Heterogeneity and Ammonium Perchlorate Gas Phase Decomposition as Composite Propellant Burning Rate Controlling Mechanisms," submitted to the Fourth ICRPG Combustion Conference, (October 1967).
12. Hightower, J. D. , Comment made at ICRPG, 2nd Combustion Conference, (November 1965).
13. Beckstead, M. W. , Personal Communication, (May 1967).
14. Markowitz, M. M. and Boryta, D. A. , "Some Aspects of the Crystallographic Transition of Ammonium Perchlorate," ARS J. 32, 1941-1942 (1962).
15. JANAF Thermochemical Data , Dow Chemical Co. , Midland, Michigan.
16. Rosser, W. A. , Inami, S. H. , and Wise, H. , "Thermal Diffusivity of Ammonium Perchlorate," AIAA Journal, Volume 4, No. 4, (April 1966), pp. 663-666.
17. Waesche, R. H. W. , Wenograd, J. , and Feinauer, L. R. , "Investigation of Solid Propellant Decomposition Characteristics and Their Relation to Observed Burning Rates," ICRPG/AIAA 2nd Solid Propulsion Conference, (June 1967), Volume of preprints published by AIAA, pp. 136-147.

UNCLASSIFIED

UNCLASSIFIED

NOMENCLATURE

<u>Latin Symbols</u>	<u>Definition</u>	<u>Unit</u>
c	specific heat	cal/gm°F
E	activation energy for pyrolysis law	cal/mole
f	fraction of reactant remaining unconsumed	
k	thermal conductivity	cal/cm sec°C
\dot{q}	energy per unit volume from chemical reactions	cal/cm ³ sec
Q	heat evolution accompanying a chemical or physical change	cal/gm
r	burning rate	cm/sec
R	gas constant	1.9867 cal/mole°K
T	temperature	°K
t	time	sec
x	normal distance from the surface	cm
Z	pre-exponential factor	

Greek Symbols

α	thermal diffusivity	cm ² /sec
λ	latent heat of crystal phase transition	cal/gm
ρ	density	gm/cm ³

Subscripts

s	solid phase surface
tr	cubic-orthorhombic interface

UNCLASSIFIED

Subscripts

Definitions

0	initial conditions of solid phase
1	cubic phase
2	orthorhombic phase

UNCLASSIFIED

CONFIDENTIAL

CONFIDENTIAL

Security Classification

DOCUMENT CONTROL DATA - R&D		
(Security classification of title, body of abstract and indexing annotation must be entered when the overall report is classified)		
1. ORIGINATING ACTIVITY (Corporate author) Thiokol Chemical Corporation Huntsville Division Huntsville, Alabama		2. REPORT SECURITY CLASSIFICATION CONFIDENTIAL 2b GROUP IV
3. REPORT TITLE Combustion Mechanism of High Burning Rate Solid Propellants (U)		
4. DESCRIPTIVE NOTES (Type of report and inclusive dates) Quarterly Technical Report, 1 June through 31 August 1967		
5. AUTHOR(S) (Last name, first name, initial) Flanigan, David A		
6. REPORT DATE September 1967	7a. TOTAL NO. OF PAGES i-iv, 1-53	7b. NO. OF REFS 17
8a. CONTRACT OR GRANT NO. F04611-67-C-0034	9a. ORIGINATOR'S REPORT NUMBER(S) AFRPL-TR-67-250	
b. PROJECT NO. 3148	9b. OTHER REPORT NO(S) (Any other numbers that may be assigned this report) Report 63-67 (Control No. C-67-63A)	
10. AVAILABILITY/LIMITATION NOTICES In addition to security requirements which must be met this document is subject to special export controls and each transmittal to foreign governments or foreign nationals may be made only with prior approval of AFRPL (RPPR-STINFO), Edwards, California 93523		
11. SUPPLEMENTARY NOTES ---	12. SPONSORING MILITARY ACTIVITY Air Force Rocket Propulsion Laboratory Research and Technology Division Edwards AFB, California 93523	
13. ABSTRACT (C) Thiokol's program to tailor the burning rate of a propellant predictably and controllably to any desired level in the range from 1 to 10 inches per second is divided into three phases: Phase I - Synthesis of Burning Rate Catalysts, Phase II - Decomposition Studies and Evaluation of Catalysts and Phase III - Decomposition of Advanced Oxidizers, Fuels, and Binders. Experiments will be performed to synthesize more efficient burn rate catalysts by maximizing already determined guideline properties toward development of an ideal catalyst under Phases I and II. Following catalyst synthesis, each compound showing potential will be subjected to comprehensive decomposition studies and combustion mechanism evaluation with propellant ingredients. Thermogravimetric analyses of catalysts mixed with HC polymer show that none of the catalysts tested appear to catalyze the decomposition of HC polymer. Propellants formulated with the copper (I) complex, the copper (II) complex and the cobalt (II) complex of 8-ferrocenyl-8-oxo-propionaldehyde demonstrated burning rates higher than that of similar propellant containing n-butyl ferrocene [PLASTISCAT-IV(R)] at the 2 percent level. An analysis to relate sub-surface heating to changes in ammonium perchlorate crystal structure was conducted. It was shown that if the concept of a constant surface temperature is valid and if the extrapolated value of thermal diffusivity is accurate to within 10 percent, the surface temperature of burning ammonium perchlorate is $440 \pm 30^\circ\text{C}$.		

DD FORM 1 JAN 64 1473

CONFIDENTIAL

CONFIDENTIAL
Security Classification

14. KEY WORDS	LINK A		LINK B		LINK C	
	ROLE	WT	ROLE	WT	ROLE	WT
Combustion mechanism Burn rate Catalyst synthesis Decomposition studies						

INSTRUCTIONS

1. **ORIGINATING ACTIVITY:** Enter the name and address of the contractor, subcontractor, grantee, Department of Defense activity or other organization (*corporate author*) issuing the report.

2a. **REPORT SECURITY CLASSIFICATION:** Enter the overall security classification of the report. Indicate whether "Restricted Data" is included. Marking is to be in accordance with appropriate security regulations.

2b. **GROUP:** Automatic downgrading is specified in DoD Directive 5200.10 and Armed Forces Industrial Manual. Enter the group number. Also, when applicable, show that optional markings have been used for Group 3 and Group 4 as authorized.

3. **REPORT TITLE:** Enter the complete report title in all capital letters. Titles in all cases should be unclassified. If a meaningful title cannot be selected without classification, show title classification in all capitals in parentheses immediately following the title.

4. **DESCRIPTIVE NOTES:** If appropriate, enter the type of report, e.g., interim, progress, summary, annual, or final. Give the inclusive dates when a specific reporting period is covered.

5. **AUTHOR(S):** Enter the name(s) of author(s) as shown on or in the report. Enter last name, first name, middle initial. If military, show rank and branch of service. The name of the principal author is an absolute minimum requirement.

6. **REPORT DATE:** Enter the date of the report as day, month, year; or month, year. If more than one date appears on the report, use date of publication.

7a. **TOTAL NUMBER OF PAGES:** The total page count should follow normal pagination procedures, i.e., enter the number of pages containing information.

7b. **NUMBER OF REFERENCES:** Enter the total number of references cited in the report.

8a. **CONTRACT OR GRANT NUMBER:** If appropriate, enter the applicable number of the contract or grant under which the report was written.

8b, 8c, & 8d. **PROJECT NUMBER:** Enter the appropriate military department identification, such as project number, subproject number, system numbers, task number, etc.

9a. **ORIGINATOR'S REPORT NUMBER(S):** Enter the official report number by which the document will be identified and controlled by the originating activity. This number must be unique to this report.

9b. **OTHER REPORT NUMBER(S):** If the report has been assigned any other report numbers (*either by the originator or by the sponsor*), also enter this number(s).

10. **AVAILABILITY/LIMITATION NOTICES:** Enter any limitations on further dissemination of the report, other than those imposed by security classification, using standard statements such as:

- (1) "Qualified requesters may obtain copies of this report from DDC."
- (2) "Foreign announcement and dissemination of this report by DDC is not authorized."
- (3) "U. S. Government agencies may obtain copies of this report directly from DDC. Other qualified DDC users shall request through _____."
- (4) "U. S. military agencies may obtain copies of this report directly from DDC. Other qualified users shall request through _____."
- (5) "All distribution of this report is controlled. Qualified DDC users shall request through _____."

If the report has been furnished to the Office of Technical Services, Department of Commerce, for sale to the public, indicate this fact and enter the price, if known.

11. **SUPPLEMENTARY NOTES:** Use for additional explanatory notes.

12. **SPONSORING MILITARY ACTIVITY:** Enter the name of the departmental project office or laboratory sponsoring (*paying for*) the research and development. Include address.

13. **ABSTRACT:** Enter an abstract giving a brief and factual summary of the document indicative of the report, even though it may also appear elsewhere in the body of the technical report. If additional space is required, a continuation sheet shall be attached.

It is highly desirable that the abstract of classified reports be unclassified. Each paragraph of the abstract shall end with an indication of the military security classification of the information in the paragraph, represented as (TS), (S), (C), or (U).

There is no limitation on the length of the abstract. However, the suggested length is from 150 to 225 words.

14. **KEY WORDS:** Key words are technically meaningful terms or short phrases that characterize a report and may be used as index entries for cataloging the report. Key words must be selected so that no security classification is required. Identifiers, such as equipment model designation, trade name, military project code name, geographic location, may be used as key words but will be followed by an indication of technical context. The assignment of links, rules, and weights is optional.